

Accepted Manuscript

Tracing river chemistry in space and time: Dissolved inorganic constituents of the Fraser River, Canada

Britta M. Voss, Bernhard Peucker-Ehrenbrink, Timothy I. Eglinton, Gregory Fiske, Zhaohui Aleck Wang, Katherine A. Hoering, Daniel B. Montluçon, Chase LeCroy, Sharmila Pal, Steven Marsh, Sharon L. Gillies, Alida Janmaat, Michelle Bennett, Bryce Downey, Jenna Fanslau, Helena Fraser, Garrett Macklam-Harron, Michelle Martinec, Brayden Wiebe

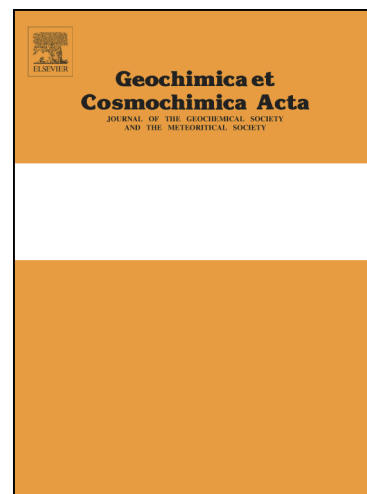
PII: S0016-7037(13)00496-1
DOI: <http://dx.doi.org/10.1016/j.gca.2013.09.006>
Reference: GCA 8442

To appear in: *Geochimica et Cosmochimica Acta*

Received Date: 9 November 2012
Accepted Date: 4 September 2013

Please cite this article as: Voss, B.M., Peucker-Ehrenbrink, B., Eglinton, T.I., Fiske, G., Wang, Z.A., Hoering, K.A., Montluçon, D.B., LeCroy, C., Pal, S., Marsh, S., Gillies, S.L., Janmaat, A., Bennett, M., Downey, B., Fanslau, J., Fraser, H., Macklam-Harron, G., Martinec, M., Wiebe, B., Tracing river chemistry in space and time: Dissolved inorganic constituents of the Fraser River, Canada, *Geochimica et Cosmochimica Acta* (2013), doi: <http://dx.doi.org/10.1016/j.gca.2013.09.006>

This is a PDF file of an unedited manuscript that has been accepted for publication. As a service to our customers we are providing this early version of the manuscript. The manuscript will undergo copyediting, typesetting, and review of the resulting proof before it is published in its final form. Please note that during the production process errors may be discovered which could affect the content, and all legal disclaimers that apply to the journal pertain.



Tracing river chemistry in space and time: Dissolved inorganic constituents of the Fraser River,
Canada

Britta M. Voss^{a,b,*} (bvoss@whoi.edu)

Bernhard Peucker-Ehrenbrink^a (behrenbrink@whoi.edu)

Timothy I. Eglinton^{a,c} (timothy.eglinton@erdw.ethz.ch)

Gregory Fiske^d (gfiske@whrc.org)

Zhaohui Aleck Wang^a (zawang@whoi.edu)

Katherine A. Hoering^a (khoering@whoi.edu)

Daniel B. Montluçon^{a,c} (daniel.montlucon@erdw.ethz.ch)

Chase LeCroy^c (chase.s.lecroy@gmail.com)

Sharmila Pal^a (muniapal@gmail.com)

Steven Marsh^c (steven.marsh@ufv.ca)

Sharon L. Gillies^c (sharon.gillies@ufv.ca)

Alida Janmaat^c (alida.janmaat@ufv.ca)

Michelle Bennett^c (michelle.bennett@student.ufv.ca)

Bryce Downey^c (bryce.downey@student.ufv.ca)

Jenna Fanslau^c (jenna.fanslau@student.ufv.ca)

Helena Fraser^c (helena.fraser@student.ufv.ca)

Garrett Macklam-Harron^c (garrett.macklam-harron@student.ufv.ca)

Michelle Martinec^c (michelle.martinec@student.ufv.ca)

Brayden Wiebe^c (brayden.wiebe@student.ufv.ca)

^a Woods Hole Oceanographic Institution, Department of Marine Chemistry & Geochemistry, 266

Woods Hole Rd, Woods Hole MA 02543, USA

^b Massachusetts Institute of Technology, Department of Earth, Atmospheric, & Planetary

Sciences, 77 Massachusetts Ave, Cambridge MA 02139, USA

^c Eidgenössische Technische Hochschule, Department Erdwissenschaften, Sonneggstrasse 5,

8092 Zürich, Switzerland

^d Woods Hole Research Center, 149 Woods Hole Rd, Falmouth MA 02540, USA

^e University of the Fraser Valley, 33844 King Rd, Abbotsford B.C. V2S 7M8, Canada

* Author to whom correspondence should be addressed:

266 Woods Hole Road, MS 25

Woods Hole MA 02543, USA

+1 508 289 2892 (office phone)

+1 508 457 2193 (fax)

Abstract

The Fraser River basin in southwestern Canada bears unique geologic and climatic features which make it an ideal setting for investigating the origins, transformations and delivery to the coast of dissolved riverine loads under relatively pristine conditions. We present results from sampling campaigns over three years which demonstrate the lithologic and hydrologic controls on fluxes and isotope compositions of major dissolved inorganic runoff constituents (dissolved nutrients, major and trace elements, $^{87}\text{Sr}/^{86}\text{Sr}$, δD). A time series record near the Fraser mouth allows us to generate new estimates of discharge-weighted concentrations and fluxes, and an overall chemical weathering rate of $32 \text{ t km}^{-2} \text{ y}^{-1}$. The seasonal variations in dissolved inorganic species are driven by changes in hydrology, which vary in timing across the basin. The time series record of dissolved $^{87}\text{Sr}/^{86}\text{Sr}$ is of particular interest, as a consistent shift between higher (“more radiogenic”) values during spring and summer and less radiogenic values in fall and winter demonstrates the seasonal variability in source contributions throughout the basin. This seasonal shift is also quite large (0.709 – 0.714), with a discharge-weighted annual average of 0.7120 (2 s.d. = 0.0003). We present a mixing model which predicts the seasonal evolution of dissolved $^{87}\text{Sr}/^{86}\text{Sr}$ based on tributary compositions and water discharge. This model highlights the importance of chemical weathering fluxes from the old sedimentary bedrock of headwater drainage regions, despite their relatively small contribution to the total water flux.

1. Introduction

1.1 Tracing river geochemistry across space and time

Elemental and isotope tracers have tremendous utility in elucidating the sources and biogeochemical history of material dissolved in river waters (e.g. Livingstone, 1963; Mackenzie and Garrels, 1966; Palmer and Edmond, 1989; Gaillardet et al., 1999; Schulte et al., 2011). Time series observations are critical in order to accurately quantify annual fluxes and understand the processes controlling the properties of chemical species in rivers (Walling and Foster, 1975; Christophersen et al., 1990; Scanlon et al., 2001; Raymond and Cole, 2003; Tipper et al., 2006; Cooper et al., 2008; Bagard et al., 2011; Kirchner and Neal, in press). In addition, basin-integrated signals often do not represent the entire drainage region equally, but rather are significantly biased by specific, sometimes geographically small, areas (Edmond, 1992; Blum et al., 1998; Hartmann et al., 2009; Wolff-Boenisch et al., 2009). Only by sampling for both spatial variability across a basin and temporal variability near a river mouth can the dynamics of source contributions and seasonal dynamics be understood.

The Fraser River basin (Fig. 1) was chosen as the focus for this work because of its large variability in bedrock geology across a relatively small area, which has been shown to impart stark contrasts to the characteristics of its chemical load (Armstrong, 1988; Cameron et al., 1995; Cameron, 1996; Cameron and Hattori, 1997). In addition, the large seasonal variability in discharge of the Fraser, typical of temperate mountainous and subarctic regions, is expected to lead to time-varying changes in the relative contributions of material derived from different portions of the basin. These properties make the Fraser basin an excellent candidate for quantitatively tracing the sources of dissolved material over time.

Studies such as this are necessary in order to (1) accurately quantify annual fluxes of terrestrial material to the coastal ocean; (2) determine the relative importance of different portions of the drainage basin to the total chemical load; (3) accurately interpret records of past fluvial drainage basin history; and (4) establish seasonal and interannual variability in natural systems under increasing anthropogenic and environmental stress. In recent centuries and decades, river basins have emerged as some of the areas most acutely affected by human influence in the forms of global warming, resource extraction, land use change, and ecosystem disturbance (Nilsson, 2005; Peterson, 2006; Chao et al., 2008; Milliman et al., 2008; Syvitski, 2008; Coggins et al., 2011). Research on large, relatively pristine systems such as the Fraser River, which are rare, is critical to the fundamental understanding of how river geochemistry evolves under natural conditions, and for projections of how this behavior may change in the future.

1.2 Fraser River basin environmental setting

A detailed description of the geological composition of the Foreland, Omineca, Intermontane, and Coast belts comprising the bedrock of the Fraser basin is given by Cameron and Hattori (1997) and references therein. The hydrology of the Fraser River is characterized by a spring freshet fed by a mixture of snowmelt and rainfall, which typically begins in April and tapers off throughout the summer, and is often followed by a secondary fall peak driven by rain storms (Fig. 2; Dorsey, 1991). Discharge during the spring freshet peaks at approximately $8000 \text{ m}^3 \text{ s}^{-1}$, while winter base flow is $\sim 1800 \text{ m}^3 \text{ s}^{-1}$. The hydrology of subbasins within the watershed is complex due to mountainous topography and variable climatic regimes (Thorne and Woo,

2011), resulting in large differences in the timing of the spring freshet in various tributary basins (Déry et al., 2012).

This study combines spatial and temporal observations of river chemistry in order to interpret seasonal patterns at the river mouth in the context of upstream inputs. We present results from three basin-wide surveys of the main stem and multiple tributaries at different hydrologic stages, as well as a two-year time series near the river mouth with samples collected approximately twice per month. Our results show how seasonal variations in hydrology coincide with changes in the flux and composition of dissolved inorganic material carried by the Fraser River. Basin-wide sampling campaigns (Table 1), probing multiple points along the main stem and at confluences of major tributaries, create a framework for interpreting the trends observed in the time series. The source-specificity of isotope tracers, particularly dissolved $^{87}\text{Sr}/^{86}\text{Sr}$, allows for quantitative provenance analysis of the time-varying contributions from different sub-basins. The focus here on dissolved inorganic components lays the foundation for a holistic understanding of biogeochemical processes in rivers extending to organic matter and suspended sediments, which are the subjects of forthcoming publications.

2. Methods

2.1 *Sample collection*

All samples were collected from river banks by extending collection devices as far as possible into the stream (typically ~3 m). Exceptions to this are main stem samples in the delta, which were collected mid-channel from on board a small boat, and samples collected at Fort Langley and New Westminster, which were collected off of a dock ~50 m from the bank. The data presented in Table 2 represent the basin-wide sampling campaigns which took place in

2009, 2010, and 2011. Table 3 presents data for the time series samples collected approximately every other week from July 2009 to October 2011 at Fort Langley and New Westminster.

Water samples were collected at each site using a combination of filtration techniques. Material remaining in water passed through these filter types is hereafter defined as “dissolved.” Water samples for nutrient and trace and major element concentrations collected in summer 2009 and as part of the time series were collected with a 0.5 L high-density polyethylene (HDPE) “dipper” (Bel-Art Scienceware), subsampled with an all-plastic (polypropylene [PP] and polyethylene [PE]) syringe, and filtered through Sterivex cartridges (Millipore, pore size 0.22 μm). Samples collected in fall 2010 and spring 2011 were filtered with a membrane cartridge filter (Pall AcroPak 500 Supor Membrane, 0.8/0.2 μm pore size). All major and trace element concentration samples were collected, unacidified, in HDPE bottles (pre-cleaned with certification by the U.S. Environmental Protection Agency). This sampling protocol has been described previously (Miller, 2009; Miller et al., 2011). Nutrient concentration samples were collected in PE scintillation vials, pre-cleaned first with laboratory soap solution, then soaked for 3 days in 10% HCl, followed by 3 rinses with Milli-Q (Millipore) water. Nutrient samples were frozen in the field and stored in the dark. Total alkalinity (TA) samples were collected by pumping water through a 0.45 μm cartridge filter into 250 mL borosilicate glass bottles; samples were immediately poisoned with 60 μL of saturated HgCl_2 solution and sealed with a greased ground-glass stopper (Dickson et al., 2007).

In order to make the results and sample archives of this work accessible to the broader community, all samples have been registered in the online System for Earth Sample Registration database (www.geosamples.org). Each sample is assigned a unique International Geo Sample

Number (IGSN) code beginning with “GRO” (Global Rivers Observatory). Registered users can search the database to retrieve sample metadata and information about archived material.

2.2 Laboratory analyses

Nutrient samples were thawed in the dark immediately prior to analysis on a four-channel AutoAnalyzer (Lachat QuickChem 8000) with standard spectrophotometric methods certified by the U.S. Environmental Protection Agency. Briefly, nitrate and nitrite (NO_3+NO_2) were measured together as azo dye after reduction in a Cu-Cd column. Phosphate (orthophosphorus) was measured as a chromophoric antimony-phosphomolybdate complex. Soluble silica (hereafter denoted SiO_2) was measured as a heteropoly blue complex. Ammonium was measured as indophenol blue via the Berthelot reaction. All samples were analyzed in duplicate and concentrations were calculated from 6-point dilution curves of standard MOOS-2 (National Research Council Canada) prepared on the day of analysis. One standard dilution was analyzed for every 5 samples. No international reference standard is available for NH_4 , hence these values are calibrated to an artificial standard prepared on the day of analysis. Instrumental detection is generally $<0.05 \mu\text{mol L}^{-1}$ for all analytes. This limit represents the lowest detectable standard dilution, which is at least 5 times higher than the blank value.

Anion concentrations (Cl , SO_4) were measured on a Dionex ion chromatography system. Approximately 5 mL of undiluted sample was injected three times on an anion column (AS15, 4 mm, with ASRS suppressor) in 65% 50 mM NaOH and 35% H_2O eluents. Standards were prepared by gravimetric dilution of SpecPure ion chromatography standards (Alfa Aesar). One Milli-Q H_2O blank and one standard dilution were injected for every 3 samples. Concentrations were calculated based on 3-point standard calibration curves using Chromeleon software,

followed by blank correction. Concentrations of Br and F were also analyzed, but results were too low to be reliably quantified.

Total alkalinity (TA) measurements were made following the methods described by Wang et al. (2013). Briefly, TA was measured with an automated titrator (AS-ALK2, Apollo SciTech) using a modified Gran titration procedure (Wang and Cai, 2004); this titration includes weak acids and anions (such as HCO_3^- , CO_2^{3-} , and deprotonated organic acids) (Morel and Hering, 1993). Sample analyses were calibrated with certified reference material from Dr. A.G. Dickson at the Scripps Institution of Oceanography. Bicarbonate (HCO_3^-) is the dominant component of alkalinity in Fraser River water, representing ~98% of the total concentration (Wang et al., in prep), so we assume here that $\text{TA} = \text{HCO}_3^-$.

Water samples for cation concentrations were prepared in a clean laboratory. An indium tracer solution and sub-boiling distilled HNO_3 (to achieve 5% acidity) were added to 1 mL of undiluted sample. Blanks were prepared in the same manner with Milli-Q H_2O ($18.2 \text{ M}\Omega \text{ cm}^{-1}$) instead of river water. Standards were prepared from dilutions of natural river water standard reference material SLRS-5 (National Research Council Canada). Samples were analyzed interspersed with blanks and standard dilutions on a Thermo Scientific Element2 single collector inductively-coupled plasma mass spectrometer (ICPMS). An argon flow nebulizer and quartz double pass (cyclonic, coupled to a Scott-type) spray chamber were used to introduce the sample to the plasma source by means of self-aspiration and the ion beam was tuned scanning U, In, and Sc. The following isotopes were analyzed and reported in this manuscript: ^{82}Kr , ^{83}Kr , ^{85}Rb , ^{86}Sr , ^{87}Sr , ^{88}Sr , ^{137}Ba , and ^{138}Ba at low mass resolution ($m/\Delta m \sim 300$); ^{42}Ca , ^{43}Ca , ^{44}Ca , and ^{48}Ca at medium mass resolution ($m/\Delta m \sim 3000$); and ^{23}Na , ^{24}Mg , ^{25}Mg , ^{26}Mg , and ^{39}K at high mass resolution ($m/\Delta m \sim 10,000$). Multiple isotopes were measured for each element whenever

possible to check for isobaric interferences; such interferences were corrected when appropriate. Concentrations were calculated based on 7-point calibration curves of standard dilutions for each element.

Major and trace element concentration samples were subsampled for strontium separation in a PicoTrace[®] clean laboratory at WHOI. Target volumes were transferred to acid-cleaned Teflon beakers, dried down, and resuspended in 3.5 N distilled HNO₃. Strontium was isolated by ion chromatography using ~300 μ L of Sr Spec resin (Eichrom, 100-150 μ m) and eluted with 7 mL Milli-Q water. Column eluents were refluxed at 80°C overnight in distilled sub-boiling concentrated HNO₃ and a few drops of 30% H₂O₂ (to remove residual organics from the resin), dried down and resuspended in 5% HNO₃. Eluents were analyzed on a Thermo Scientific Neptune multicollector (MC) ICPMS by static measurement of ⁸²Kr, ⁸³Kr, ⁸⁴Sr, ⁸⁵Rb, ⁸⁶Sr, ⁸⁷Sr, and ⁸⁸Sr. Raw ⁸⁷Sr/⁸⁶Sr for all samples and standards was corrected for instrumental mass bias with a power law and corrected for ⁸⁶Kr and ⁸⁷Rb interferences. Sample results were normalized to repeated measurements of international standard SRM 987 (U.S. National Institute of Standards and Technology), analyzed once for every 5 samples. The certified value of the standard is ⁸⁷Sr/⁸⁶Sr = 0.710240; the average measured value was 0.71028 (n = 52, 2 s.d. = 0.00007). Although greater precision for this measurement is possible, the instrument was tuned to achieve the best precision for our measurements given the amount of analyte.

Stable isotope compositions of hydrogen (δ D) and oxygen (δ^{18} O) in filtered water samples were measured on a Picarro L2120-I cavity ring-down spectrometer at the ETH in Zürich, Switzerland. Each sample was injected six times, with the results of the first three injections discarded to eliminate instrumental memory effects. Results were also rejected if the concentration of H₂O was outside 20,000 \pm 2,000 ppm. Aliquots of standard reference materials

SLAP2, GISP, and VSMOW2 (International Atomic Energy Agency) were analyzed to bracket sets of 5 samples, with standard calibration corrections and interfering contamination from dissolved organic matter assessed using Picarro ChemCorrect software.

Statistics on analytical precision and accuracy for all of the above measurements are summarized under the corresponding results at the bottom of Table 2.

2.3 Discharge data and flux calculations

Daily water flux (discharge) data were obtained online from the Environment Canada Water Office (<http://www.wateroffice.ec.gc.ca>). Discharge at the city of Mission is considered the total Fraser River discharge, as this site is only 75 km from the Strait of Georgia and includes all major tributaries. A continuous record of discharge at Mission from Environment Canada (station 08MH024) is not available. Various linear correlations between reported daily discharge (Q_w) at Mission and Hope (station 08MF005) have been developed, as the station at Hope integrates discharge from the Fraser River basin above the floodplain and has a record extending back to 1912. A published calibration based only on peak flows between 1965 and 2008 (Northwest Hydraulic Consultants, 2008) reported the correlation: $Q_w^{\text{Mission}} = 1.142 * Q_w^{\text{Hope}} - 135 \text{ (m}^3 \text{ s}^{-1}\text{)}$. A calibration including the full period of overlap for Hope and Mission records yields the correlation ($r^2 = 0.983$, $n = 10,598$):

$$Q_w^{\text{Mission}} = 1.086 * Q_w^{\text{Hope}} + 344 \text{ (m}^3 \text{ s}^{-1}\text{)} \quad (1)$$

Total Fraser River discharge can alternatively be estimated by summing measured discharge at Hope with measured discharge from the Harrison River (station 08MG013). This summation estimate shows good overall agreement with the correlation estimate of Eq. 1 ($r^2 = 0.998$, $n =$

21,991). Because the correlation estimates tend to overestimate baseflow discharge, the summation estimate of total Fraser discharge has been applied for flux calculations in this study.

Environment Canada gauging data are reported online in real-time and published annually as historical data after quality control measures—necessary adjustments to rating curves based on occasional discharge measurements—have been made. Historical data for our Fraser River sites were only available through 2010. Therefore, discharge data presented here for 2011 are based on real-time data, which have been quality-checked by the authors to ensure that records do not exhibit discontinuities and are consistent with historical trends. No such issues were identified, except in the cases of the McGregor River and the Fraser River at McBride. For these sites, real-time values for 1 January through ~25 April 2011 are erroneously high (2 – 5x greater than historical average flows during this period). The McGregor and McBride sites exhibit consistent winter base flow in historical records; therefore, in these cases, an average base flow value has been applied. This issue is discussed in section 4.4 regarding the modeled time series.

2.4 Load and average concentration estimates

Annual fluxes and discharge-weighted average concentrations of dissolved species were calculated using the Load Estimator (LoadEst) program developed by the United States Geological Survey (Runkel et al., 2004). Time series measurements (“quality data”) at Fort Langley and New Westminster between September 2009 and October 2011 were used with discharge data at Mission (“flow data”) as a calibration set. Data files were manipulated using the LoadRunner program (Booth et al., 2007). Dissolved inorganic elements and isotopes are characterized with ~80 observations spanning the entire sampling period. Nutrient

concentrations are represented by 66 measurements between March 2010 and October 2011. A smaller number ($n = 13$) of TA measurements were also made on time series samples, primarily in 2011.

Annual fluxes (loads) of each constituent are presented with uncertainties of one standard deviation for the result of the three annual estimates (2009, 2010, 2011) using the maximum likelihood estimation model. This statistic thus represents a combination of year-to-year variability in fluxes and the uncertainty of calibrating the estimates from uneven sampling distributions (as samples were not collected at regular intervals of time or discharge). Variability in flux from one year to the next is expected, given differences in discharge volume. Though imperfect, the values obtained by weighting a time series record in this manner are much more robust than extrapolations based on the single or seasonal measurements commonly available for river systems.

Average river nutrient concentrations were also calculated from the Global Nutrient Export from WaterSheds (NEWS 2) model dataset (Mayorga et al., 2010). Global dissolved silicon, nitrogen, and phosphorus loads were calculated from the sum of the 5,917 exorheic basins in the dataset (version 1.0, Aug. 2011), yielding fluxes of 143×10^{12} g Si a^{-1} , 22.8×10^{12} g N a^{-1} , and 1.64×10^{12} g P a^{-1} . Actual global exorheic water discharge was calculated from the dataset in the same manner, resulting in a total of 37.9×10^3 km³ a^{-1} , which is consistent with other literature estimates, e.g. 38.3×10^3 (Fekete et al., 2002), 38.9×10^3 (Peucker-Ehrenbrink et al., 2010). Inorganic nutrient fluxes estimated by the NEWS 2 model for the Fraser River are 68.7×10^9 g Si a^{-1} , 20.5×10^9 g N a^{-1} , and 0.777×10^9 g P a^{-1} for a water flux of 102 km³ a^{-1} .

3. Results

3.1 Major and trace elements and nutrients

Concentrations of all dissolved species varied significantly at different sites across the basin, as well as at individual sites at different flow stages (Table 2). Concentrations of dissolved major (HCO_3 , Ca, Mg, SO_4 , Na, Cl, K) and trace (Sr, Ba) constituents measured at low discharge (fall 2010) are generally slightly higher than those measured at medium (summer 2009) and high (spring 2011) discharge.

Dissolved concentrations and isotope compositions of time series samples are shown in Table 3. This record demonstrates the kinetic-limited weathering behavior of most dissolved elements on the basin-scale (West et al., 2005), with only modest dilution occurring when discharge exceeds base flow (Fig. 3). Discharge-weighted average concentrations and annual fluxes of major and trace elements estimated using LoadEst are shown in Table 4. Differences in total water flux for the three years analyzed (87, 84, and 117 km^3 in 2009, 2010, and 2011, respectively) drive the observed variation in estimated fluxes of dissolved species from year to year. Concentrations reported elsewhere for the Fraser River, and for world average river water, are presented in Table 4 for comparison.

The major element concentrations in Table 4 sum to give an average total dissolved solids concentration of 74 mg L^{-1} . Scaled to the basin area and average annual discharge, this yields a chemical weathering rate of 32 $\text{t km}^{-2} \text{y}^{-1}$ for the Fraser basin. This is a minimum estimate, as the total Fraser basin area includes the entire Nechako River basin, and a significant portion of the flow of the Nechako is diverted to a different watershed for hydropower production. This diversion causes a ~3% reduction in the total natural Fraser River discharge at Hope (Dorcey, 1991).

A charge balance of major ions (HCO_3 , Ca, Mg, SO_4 , Na, Cl, K) in Table 2 indicates a slight surplus of positively charged species in nearly all samples (average +4%). The “missing” negative charge ($\sum^{\text{net}} > 0$) in most samples is likely derived from organic acids, as proposed by Spence and Telmer (2005). This is especially likely as the most positive \sum^{net} values generally occur in samples collected during the 2011 freshet, when dissolved organic carbon concentrations are likely highest. Missing positive charge ($\sum^{\text{net}} < 0$) in some tributary samples during low discharge conditions may result from unaccounted-for cations from hydrothermal (Bridge and Chilcotin rivers) or industrial (Bridge, Quesnel, and Thompson rivers) sources.

In general, concentrations of dissolved nutrients (NO_3+NO_2 , NH_4 , SiO_2 , and PO_4) were highest during the freshet sampling of spring 2011 and lowest during the low-flow sampling of fall 2010 (Table 2). Also striking are variations between different sites within the basin. The Blackwater River, for instance, exhibited consistently higher concentrations of dissolved SiO_2 than all other tributaries during any of the sampling expeditions (>2 times higher than any other site). Tributaries in the upper canyon area (Nechako, Blackwater, Chilcotin) have generally higher dissolved SiO_2 concentrations than the rest of the basin. The upper canyon region also exhibits lower NO_3+NO_2 concentrations than the rest of the basin. The time series records of nutrients show generally counterclockwise hysteresis behavior at discharge conditions above base flow (Fig. 4), cycling between relatively low concentrations during the rising limb of the freshet, followed by higher concentrations during the falling limb.

3.2 *Isotope composition of spatial tracers*

The geologic diversity and hydrologic regime of the Fraser basin lead to such distinct isotope signatures in material carried by the river, that these constituents can be viewed as

“tracers” of particular regions or even specific tributaries. Here we focus on two such tracers: the deuterium composition of water (δD), as a qualitative indicator of the precipitation source of runoff, and the dissolved radiogenic strontium composition ($^{87}\text{Sr}/^{86}\text{Sr}$), as a quantitative indicator of the lithological source of dissolved weathering products.

To a first order, the δD composition of precipitation in the Fraser basin is affected by the cumulative fractionation between ^1H and ^2H (D) of precipitation as air masses originating over the Pacific Ocean migrate inland (Gimeno et al., 2012). Year-to-year variations in the sources of air masses lead to modest variability in the average annual δD composition of precipitation in this region (Liu et al., 2011). The δD composition of precipitation approaching the Fraser basin from the west is approximately $-71 \pm 9\text{‰}$, based on monitoring at Victoria, B.C. (48.65°N , 123.43°W ; IAEA/WMO, 2006). The result of the inland movement of Pacific Ocean moisture is a progressive decrease in the δD values of regions draining the Coast Range to the Cariboo Mountains to the Rocky Mountains, or, roughly, moving upstream. Evaporation may also generate higher δD values in river water relative to precipitation, particularly in relatively arid tributary basins such as the Nechako, Blackwater, Chilcotin, and Thompson Rivers.

The magnitude of the deuterium depletion in the Fraser headwaters relative to the mouth is large, $>50\text{‰}$ between the Pitt River ($\delta D: -95\text{‰}$) and the Fraser at Fitzwilliam ($\delta D: -150\text{‰}$) (Fig. 5A). As a larger portion of the basin-integrated runoff is sourced from headwater snowmelt during the spring freshet, the time series record of δD shows a shift towards more negative isotope values at this time of year, and less negative values in fall and winter (Fig. 5B). Large variability in tributary δD composition at different flow stages complicates the interpretation of this cycle. Time series observations of the δD composition of precipitation across the basin would be needed in order to quantitatively model time-varying trends in the basin-integrated

stable isotope composition of the river. The discharge-weighted average compositions of the Fraser River based on our time series are $-126.3 \pm 3.7\text{‰}$ (δD) and $-16.63 \pm 0.49\text{‰}$ ($\delta^{18}\text{O}$) (± 1 s.d.).

Radiogenic $^{87}\text{Sr}/^{86}\text{Sr}$ in river systems is primarily influenced by bedrock age, lithology, and weathering history (Goldstein and Jacobsen, 1987; Peucker-Ehrenbrink et al., 2010; Bataille and Bowen, 2012). Lithology (with characteristic Rb/Sr composition) and bedrock age (controlling ingrowth of radiogenic ^{87}Sr from decay of ^{87}Rb) determine the amount of radiogenic ^{87}Sr in the bedrock, and chemical weathering rates determine the specific flux (or yield) of dissolved Sr from each lithology within a catchment. A basin with easily weathered sedimentary rock of old age, such as the uppermost catchment of the Fraser in the Yellowhead Lake area, has a high yield of radiogenic Sr; in contrast, a basin such as the Harrison, composed of young, more weathering-resistant igneous rock, carries a relatively low yield of less radiogenic Sr.

The correlation between drainage basin bedrock age and riverine dissolved $^{87}\text{Sr}/^{86}\text{Sr}$ has been described for many rivers; the Fraser shares with Himalayan rivers an unusually radiogenic isotope composition for the average bedrock age of its drainage basin (Peucker-Ehrenbrink et al., 2010). This likely reflects the strong influence of highly radiogenic lithologies in the headwater region with Neoproterozoic and Paleozoic (250 – 1000 Ma) strata. The ages of these strata, and not those of the Meso- and Paleoproterozoic (1000 – 2500 Ma) precursor materials (Armstrong, 1988; Cameron and Hattori, 1997), are used to calculate average bedrock ages. While the bedrock ages record this rejuvenation, the radiogenic isotope systems were not fully reset (Peucker-Ehrenbrink et al., 2010; their Fig. 7) and reflect—in part—the time-integrated history of the older material. Alternatively, old, radiogenic source areas may contribute

disproportionately to the dissolved load, due to differences in mineralogy, hydrology, or other factors.

The diversity of bedrock lithology and spatial variations in precipitation patterns within individual tributary basins are small enough that the $^{87}\text{Sr}/^{86}\text{Sr}$ compositions of these basins do not change significantly on a seasonal basis (Fig. 6). Hence, changes in the basin-integrated $^{87}\text{Sr}/^{86}\text{Sr}$ signature measured at a downstream site can be interpreted as a response to changes in the relative contributions of constant end-members. The time series record of the basin-integrated $^{87}\text{Sr}/^{86}\text{Sr}$ of the Fraser River indicates such a seasonal cycle (Fig. 7). In fall and winter, the $^{87}\text{Sr}/^{86}\text{Sr}$ composition is less radiogenic (~ 0.709), but becomes more radiogenic (~ 0.714) at the onset of the spring freshet, and remains so through late summer, months after the water flux has returned to near base flow. A secondary discharge peak in early fall is evident in both years of the record, which appears to prolong the radiogenic signature after the freshet has ended.

In addition, the magnitude of the shift from less radiogenic fall/winter $^{87}\text{Sr}/^{86}\text{Sr}$ to more radiogenic spring/summer $^{87}\text{Sr}/^{86}\text{Sr}$ is not equivalent in both years of the record. The freshet of 2011 was larger with a more rapid onset than that of 2010; however, the change in $^{87}\text{Sr}/^{86}\text{Sr}$ was smaller during the 2011 freshet. On a finer temporal scale, this time series record also shows that the period when the balance of radiogenic versus unradiogenic contributions is shifted most strongly towards less radiogenic character is very short (on the order of two weeks). This point was captured by one or two samples in late fall each year; therefore, the true minimum value may have been even lower than what was observed.

Using the LoadEst program, a discharge-weighted $^{87}\text{Sr}/^{86}\text{Sr}$ value was calculated by translating the time series record of Sr concentrations and dissolved $^{87}\text{Sr}/^{86}\text{Sr}$ values to

concentrations of the individual isotopes ^{87}Sr and ^{86}Sr , accounting for changes in the atomic weight of Sr. The discharge-weighted flux of ^{87}Sr was divided by that of ^{86}Sr , resulting in a dissolved $^{87}\text{Sr}/^{86}\text{Sr}$ value for the Fraser River of 0.7120 (2 s.d. = 0.0003).

4. Discussion

4.1 Seasonally-integrated flux estimates

The vast majority of flux or average concentration estimates for global rivers are based on very few measurements; many data are decades old and represent a single and often biased portion of the river's hydrograph. The oft-cited global compilation of major element concentrations of Meybeck (1979), for instance, includes discharge-weighted concentrations for only 10 of the world's largest rivers, while the remaining 18 rivers are represented by arithmetic means of 20 or fewer measurements. In the case of the Fraser, the values reported by Meybeck (1979) (which are reproduced in the compilation of Berner and Berner, 1996) derive from three samples during medium and low discharge collected at the city of Mission in 1958-59 (Durum et al., 1960). These data are also the ultimate source of Fraser values reported in a more recent well-known compilation by Gaillardet et al. (1999), based on the GEMS-GLORI database (Meybeck and Ragu, 2012), together with Sr concentration and isotope composition from the study of Cameron et al. (1995). However, the Sr data of Gaillardet et al. (1999) do not correspond to any of the values reported in the Cameron et al. (1995) work, nor to other previously published data (Wadleigh et al., 1985; Cameron, 1996; Cameron and Hattori, 1997). Thus reference to such global compilations should be made cautiously.

Another well-known global compilation from Livingstone (1963) includes major element concentrations for the Fraser and world average river water (Table 4). The Fraser values in this

collection are based on a single sample from December 1938, and correspondingly show higher concentrations of most solutes, as expected for low discharge conditions (winter). A more recent study of the Fraser River by Spence and Telmer (2005) extrapolates measurements at two flow stages to estimate annual fluxes by simply assuming that medium and low flow conditions represent 70% and 30% of total discharge, respectively.

The fact that the discharge-weighted fluxes of all dissolved elements in the Fraser considered here scale proportionally with discharge gives promise for the determination of more accurate flux estimates in rivers with only water flux monitoring, once this relationship has been calibrated. The time series presented here for the Fraser provides a template for the frequency of sampling necessary to capture the variability in a highly dynamic system, which may provide a benchmark for future work in other basins.

4.2 Sources of dissolved inorganic material

The predominance of HCO_3^- , Ca, Mg, and Si in the dissolved load point to the action of silicate and carbonate weathering within the Fraser basin (Fig. 8). Relatively low Na and Cl concentrations (compared to the global average, see Table 4) demonstrate a lack of significant pollution (e.g. pulp and sewage effluent, road salt), inputs from evaporite weathering, or hydrothermal sources. The ratios of major elements in tributaries of the Fraser all fall on a mixing line between carbonate- and silicate-dominated regimes. Main stem sites follow a path from the carbonate towards the silicate end-members moving from the headwaters to the delta. The influence of carbonates is mainly confined to headwater regions, and the silicate lithologies that dominate the remainder of the basin dilute the carbonate signal as water flows downstream. This observation is consistent with the regional geology. Fraser River waters are generally

slightly undersaturated with respect to calcite (Wang et al., in prep). The influence of pulp mill effluent on Na and Cl concentrations in the Fraser near the confluence with the Nechako River has been demonstrated (Cameron, 1996); however, this flux is not detectable as far downstream as our time series location (Spence and Telmer, 2005).

The presence of Cl in unpolluted, evaporite-free river water unaffected by hydrothermal springs is indicative of the incorporation of sea salt aerosols (so-called cyclic salts) (Meybeck, 1987; Meybeck and Helmer, 1989). The importance of this source of Cl to the Fraser River is supported by the increase in concentration in the main stem moving from the inland, mountainous headwaters towards the Pacific Ocean. There may be an additional source of Cl and other dissolved species from hydrothermal springs in metamorphic lithologies of the Coast Range, particularly in the Pitt and Harrison rivers (Friele and Clague, 2009), as has been shown in some catchments of the Himalaya (Galy and France-Lanord, 1999; Becker et al., 2008) and the Yellowstone River (Hurwitz et al., 2010). Assuming such hydrothermal inputs are negligible and sea salt aerosols are the sole source of Cl measured at the time series sampling site, the sea salt aerosol contribution to other dissolved concentrations can be calculated using seawater elemental ratios to Cl. Applying this calculation to the discharge-weighted average concentrations in Table 4 shows that sea salt aerosols contribute little (<3%) to the observed levels of most major ions, with the exception of Na, which is 26% sea salt-derived. The time series samples show a peak in the sea salt contribution during fall and winter relative to spring and summer, pointing to an increase in the relative importance of the precipitation source of dissolved species during low discharge periods. Individual sites with a calculated sea salt contribution >100% (such as SO₄ in the Pitt River) suggest additional sources of Cl, such as hydrothermal springs.

One sample from January 2011 (GRO000117, Table 3) shows a sharp peak in absolute concentrations of most major and some trace solutes, notably excluding Ca, SiO₂, and Ba. Chloride and Na exhibited 157x and 43x enrichments, respectively, over their discharge-weighted average concentrations, while other solutes were 2 – 7x their average values. This is likely due to a pulse of concentrated fluid into the Fraser River near the sampling site (e.g. road salt runoff, sewage overflow, industrial release). The pulse was short-lived, as the following sample (9 days later) shows no elevated concentrations. A road salt source is most likely, as this sample was collected during a significant winter snow storm. Analysis of rainwaters from across the basin and records of road salting would further inform the importance and nature of sea salts to variability of the Fraser River dissolved load.

4.3 Global and historical context of current results

Comparing our discharge-weighted concentrations (Table 4) to those in global “average” river water, the Fraser is relatively dilute in many solutes (SiO₂, Na, Cl, NO₃+NO₂, PO₄, and Ba) and typical in others (Ca, Mg, SO₄, K, Sr). In addition to the global average river compilations described above, Table 4 also includes values from recent assessments by Peucker-Ehrenbrink et al. (2010) and Miller et al. (2011), which calculate average river water compositions from a database of observations spatially extrapolated using a large-scale drainage region approach (Graham et al., 1999).

To compare our results to the study of Cameron (1996), which is based on an Environment Canada time series record from 1984 – 1992, we focus on his most downstream main stem sampling site at Hope. It should be noted, however, that our estimates are based on samples collected 100 km further downstream and after the confluence of the Harrison River, a

large tributary (~15% of total discharge) with low concentrations of dissolved material. The average values reported by Cameron (1996) for Hope are within $\pm 30\%$ of our discharge-weighted average concentrations. Exceptions include Cl, which is 2 times higher than our estimate, and NO_3+NO_2 , for which our estimate is ~4 times higher. The apparent drop in Cl load in the Fraser is likely due to changes in organohalide pollution standards for pulp mills in the basin, which began in 1992. Our comparatively high NO_3+NO_2 concentrations are likely due to the fact that our sampling site at Fort Langley includes runoff from the Fraser Valley agricultural region. The variability in nutrient concentrations at different sites across the basin may be due to a combination of hydrologic processes (surface runoff, groundwater discharge, flushing of soils, and dilution) and biogeochemical effects (turbulence, light penetration, availability of micronutrients, and temperature impacts on biological activity). For instance, Cameron (1996) attributes the pulse of NO_3+NO_2 during the early freshet to mobilization of NO_x aerosols accumulated in winter snowpack.

Although rich for its length, the Environment Canada record presented by Cameron (1996) is complicated by the use of different methods over time. Prior to 1990, samples were filtered (0.45 μm) and analyzed by atomic absorption spectrometry or flame photometry; later samples were not filtered but subjected to a weak acid leach (termed “extractable”) and analyzed by ICP-emission spectroscopy. Quality analysis by the authors resulted in exclusion of SiO_2 data predating the change, citing “substantially different results” (Cameron, 1996). Trace element concentrations (Sr and P) were based on strong acid leaching of unfiltered samples, and also underwent a change in analytical methods in 1990. It is therefore difficult to compare our data (from 0.22 μm filtered, unacidified samples) with those that may have elevated solute concentrations from acid-leaching of suspended sediments. Finally, average concentrations

reported by Cameron (1996) are mean values of regularly spaced samples, which will over-represent low-discharge periods (when concentrations are higher), resulting in higher concentrations than a true discharge-weighted average.

Also shown in Table 4 are concentrations calculated from annual fluxes generated by the global Nutrient Export from Watersheds (NEWS 2) model, developed to estimate regional- and continental-scale nutrient fluxes to the ocean (Dumont et al., 2005; Harrison et al., 2005; Seitzinger et al., 2005; Beusen et al., 2009; Mayorga et al., 2010). Compared to the NEWS-estimated global average concentrations, NEWS-estimated Fraser nutrient concentrations are very low in dissolved inorganic N, P, and Si. It is important to note, however, that the NEWS models are tuned to match large-scale flux estimates. Scaling down to a drainage area the size of the Fraser is likely to lead to large uncertainties. The NEWS nitrogen model also does not distinguish between NO_3/NO_2 and NH_4 .

The NEWS-estimated Fraser nutrient concentrations agree rather poorly with our discharge-weighted estimates (showing lower SiO_2 and higher PO_4 and NO_3+NO_2). The NEWS model parameterizes nutrient fluxes based on land uses, including agricultural and urban sources. Our time series sampling location drains only ~60% of the agricultural lands in the Fraser floodplain (Brisbin, 1994), and, importantly, lies entirely upstream of any inputs from the Vancouver metropolitan area. Our measurements may exclude significant inputs of N and P from fertilizer and manure runoff and sewage and stormwater overflow, sources which rival or dwarf natural fluxes in many other rivers (Howarth et al., 1996; Boyer et al., 2006; Shen and Liu, 2008; Alvarez-Cobelas et al., 2009). If inputs in the Vancouver area downstream of Fort Langley account for the discrepancy between the NEWS model nutrient flux estimates and our

discharge-weighted estimates, then urban sources represent ~61% of the dissolved inorganic nitrogen and ~52% of the dissolved inorganic phosphorus fluxes of the Fraser River.

The influence of groundwater seepage on concentrations of dissolved solutes in the Fraser River is unknown and requires further study. However, the large seasonal variation in the δD time series record suggests that groundwater is not a significant source of water (and therefore dissolved material) to the river compared to surface runoff. More data are needed on the seasonal variability in precipitation composition across the basin in order to quantify the importance of this potential source (for example, as demonstrated by Calmels et al., 2011).

Literature values of $^{87}\text{Sr}/^{86}\text{Sr}$ available for the Fraser River (Table 5) are variable; however, the differences can be understood in the context of the time series presented here. Wadleigh et al. (1985) report a value of 0.71195 for a sample collected in May 1979, and Cameron and Hattori (1997) report 0.712707 for a sample collected in July 1993. These results align well with the values observed in our time series (Fig. 7): ~0.7115 in May, and ~0.7128 in July. A third Fraser River $^{87}\text{Sr}/^{86}\text{Sr}$ literature value, 0.7188 reported by Allègre et al. (2010), is significantly more radiogenic than all other reported values, and more radiogenic than any individual value observed in our time series record. This value, although cited as unpublished data, likely derives from the dissolved $^{87}\text{Sr}/^{86}\text{Sr}$ value of 0.718886 reported by both Millot et al. (2003) and Huh et al. (2004) for a Fraser main stem sample (CAN99-21) collected at the city of Prince George. This site is located between our main stem sampling sites of Hansard and Stoner, which exhibited $^{87}\text{Sr}/^{86}\text{Sr}$ of ~0.719 in our analyses. It therefore appears that the “Fraser” value reported by Allègre et al. (2010) reflects not the entire Fraser River, but merely the upper third of the basin. These observations highlight the danger of assigning single literature values as

representative averages for an entire system, and the importance of seasonal sampling for large river systems such as the Fraser.

4.4 Modeling seasonal variability in dissolved load composition

The seasonal trend observed in the time series $^{87}\text{Sr}/^{86}\text{Sr}$ record demonstrates that, although the total Fraser River hydrograph can serve as an indicator of when upstream portions of the drainage basin begin to exert a stronger influence on the composition of the dissolved load, it is not quantitatively informative about the duration or magnitude of this shift. To better elucidate the observed variability in $^{87}\text{Sr}/^{86}\text{Sr}$ composition in the time series record, we have constructed a model to predict the composition at the Fort Langley site based on chemical and hydrological inputs upstream. The model is an isotope mixing equation, which sums the contributions of eight major tributary basins (Thompson, Nechako, Harrison, Quesnel, Chilcotin, McGregor, Blackwater, and the Fraser upstream of McBride) to the main stem of the Fraser. For each basin, we applied a single value of Sr concentration, $^{87}\text{Sr}/^{86}\text{Sr}$ composition, and daily discharge from Environment Canada online real-time records. Discharge for each model day represents a 7-day running average, i.e. the mean of the daily discharge values for the 7 day period centered on a given model day. The equation has the form:

$$R_{\text{mix}} = \frac{\sum_i (R_i C_i Q_i)}{\sum_i (C_i Q_i)} \quad (2)$$

where R is the $^{87}\text{Sr}/^{86}\text{Sr}$ composition, C_i is the Sr concentration, and Q_i is the water flux of tributary i . We have assumed that the Sr concentration and $^{87}\text{Sr}/^{86}\text{Sr}$ composition for each tributary are invariant, and that changes in the atomic weight of strontium, groundwater contributions (e.g. Calmels et al., 2011), and water abstractions can be neglected. Differences in

Sr concentration for tributaries were somewhat variable during the three sampling campaigns (Fig. 9); however, the differences did not follow a pattern suggesting dilution at different flow stages. We therefore chose to use the average Sr concentration from the three flow stages. As shown earlier (Fig. 6), the $^{87}\text{Sr}/^{86}\text{Sr}$ composition of these tributaries was essentially constant at low, medium, and high flow. These approximations are appropriate for the purposes of this model; lacking time series measurements on individual tributaries, attempting to interpolate seasonality in these properties could lead to spurious results.

Due to irregularities in certain portions of Environment Canada real-time discharge records, we chose to adjust discharge values for specific periods. For the McGregor River and Fraser at McBride gauging stations (Environment Canada stations 08KB003 and 08KA005, respectively), real-time data for January – April 2011 are abruptly and extremely high, inconsistent with the ~60-year historical records at these sites. For the purposes of our model, we applied a constant discharge of $35 \text{ m}^3 \text{ s}^{-1}$ for both sites, which is consistent with historical winter base flow. The timing of the transition from base flow to freshet (which is rapid at both sites) is difficult to constrain, which may generate a discontinuity in modeled $^{87}\text{Sr}/^{86}\text{Sr}$ during the early freshet period in 2011.

The model clearly captures the observed seasonal shift between relatively radiogenic and unradiogenic $^{87}\text{Sr}/^{86}\text{Sr}$ composition, both in timing and magnitude (Fig. 10). Shorter timescale changes are also apparent, most notably the dip towards a less radiogenic signature in late summer, before the return to more radiogenic values during the secondary fall discharge peaks in 2009 and 2011. Overall the seasonal trends predicted by the model match the time series observations.

There are, however, notable divergences between the model and the measured $^{87}\text{Sr}/^{86}\text{Sr}$ values. Two main disparities stand out: the model is at nearly all times more radiogenic than the measured values, and the offset between the model and the observations is systematically larger at certain times of year. The first issue, regarding a bias in the spatial representativeness of the modeled tributaries is addressed in Figure 11, which shows the percentage of the total water flux characterized by our modeled tributaries. The times of year when the model captures the greatest fraction of the total discharge is during the spring freshet and summer, when $^{87}\text{Sr}/^{86}\text{Sr}$ is most radiogenic. During late fall and winter, the model gradually loses predictive power as a smaller portion of the discharge falls inside the window of the monitored gauging stations (as little as 40%). This is related to the second issue of the consistently radiogenic bias of the model, in that upstream subdrainage basins exert more influence during the spring and summer months than during late fall and winter; thus, the larger fraction of uncharacterized discharge during fall and winter may also have a less radiogenic signature than that during spring and summer. In addition, the model captures less of the actual discharge during the 2011 freshet than during the 2010 freshet, which may explain the greater offset between our model and observations in 2011 versus 2010.

To address these issues, we consider that the eight modeled tributaries do not constitute the entire drainage basin, and appear to be consistently biased towards a more radiogenic subset of the total discharge. Accounting for the hundreds of very small basins which comprise the remaining 10 to 60% of the total discharge with additional measurements of $^{87}\text{Sr}/^{86}\text{Sr}$ and water flux is an unrealistic goal. However, it is clear that the model tends to be biased towards more radiogenic contributions. Assuming that the unradiogenic portions of the basin contribute the entirety of the “missing” component in our model, we can add such a component to account for

the uncharacterized fraction of the total discharge. Tributaries contributing Sr with a less radiogenic signature are represented by basins draining the Coast Range: Nechako, Blackwater, Chilcotin, Bridge, Harrison, and Pitt Rivers. These tributaries have consistently less radiogenic $^{87}\text{Sr}/^{86}\text{Sr}$ (0.7043 – 0.7049) and low Sr concentration (0.13 – 0.81 $\mu\text{mol L}^{-1}$). Applying a Sr concentration of 0.45 $\mu\text{mol L}^{-1}$ and $^{87}\text{Sr}/^{86}\text{Sr}$ composition of 0.7046 to the unmonitored basins results in a modified model shown in Figure 12. The discharge of the missing component is calculated as the difference between total Fraser River discharge and the sum of the discharges of each modeled tributary. The addition of this missing component aligns the model much more closely with the observed $^{87}\text{Sr}/^{86}\text{Sr}$ values throughout the record, suggesting that the Coast Range is the source of nearly all of the uncharacterized Sr flux in the basin. This conclusion is supported by the fact that tributary basins in the lower portions of the watershed (mainly draining the Coast Range) experience more significant secondary fall discharge peaks than basins draining the upper portions of the watershed.

There are still points where the modified model and the measured values diverge. In the first months of 2010, as the measured $^{87}\text{Sr}/^{86}\text{Sr}$ begins to rise after its fall 2009 minimum, the modified model predicts a longer persistence of less radiogenic values than is observed in the samples (Fig. 12). The points where the modified model predicts the least radiogenic values correspond to brief discharge peaks. This may be due to the fact that these winter peaks contain a significant flux from radiogenic portions of the basin in addition to the unradiogenic flux assumed for the missing component. In contrast, the recovery from the minimum $^{87}\text{Sr}/^{86}\text{Sr}$ in early 2011 shown by the modified model matches the observed values much more closely. There appear to have been fewer large discharge pulses during this period in 2011 than in 2010, and the assumption of a missing component made of exclusively unradiogenic Sr is more

appropriate for 2011. The divergence between the modified model and measured values at the onset of the 2011 freshet is likely related to our imprecise estimates of discharge for the McGregor and McBride drainages during the transition between base flow and freshet conditions.

An alternative approach to this type of analysis is to define the composition of end-members and solve for their relative contributions through time. For instance, Calmels et al. (2011) modeled the relative contributions of various reservoirs (slow and rapid surface runoff and deep groundwater) within the Liwu River in Taiwan during a typhoon event. Their analysis found a consistent offset to less radiogenic $^{87}\text{Sr}/^{86}\text{Sr}$ values of the model relative to measured values, attributed to unrepresentative characterization of deep groundwater. Our Sr model assumes that the contribution of each source (tributary flux) is known, and the ability of the modeled $^{87}\text{Sr}/^{86}\text{Sr}$ to predict the observed values indicates that these sources do represent the major contributors to the total dissolved load of the Fraser. The calculated composition of the uncharacterized portion of the discharge suggests additional sources with, on average, composition similar to that of Coast Range tributaries.

Despite the apparently better agreement between the modified model curve shown in Figure 12 and the original curve in Figure 10, assuming an entirely Coast Range-like composition for the missing discharge overcompensates for the radiogenic bias of the original model. Figure 13A compares the results of the two models to the measured time series values. The magnitude of the less radiogenic offset of the modified model is nearly as large as the more radiogenic offset of the original model. By adjusting the $^{87}\text{Sr}/^{86}\text{Sr}$ composition of the missing discharge component, we can estimate the composition necessary to bring the modified model closest to 1:1 agreement with the measured time series values. The best agreement (determined

as the minimum residual sum of squares, i.e. the sum of the squared difference between each measured time series value and the model estimate for the same day) occurs at $^{87}\text{Sr}/^{86}\text{Sr} = 0.7080$ with the residual sum of squares = 5.5×10^{-5} (Fig. 13B). Assuming this composition is the product of a binary mixture of a radiogenic Rocky Mountain endmember with $^{87}\text{Sr}/^{86}\text{Sr} = 0.7285$ and an unradiogenic Coast Range endmember with $^{87}\text{Sr}/^{86}\text{Sr} = 0.7046$ (based on our measurements of tributaries in these regions), we estimate that the missing strontium is derived of ~14% Rocky Mountain material and ~86% Coast Range material. In reality, these proportions represent sources from across the basin and likely fluctuate throughout the year. This complexity cannot be resolved without more detailed spatial and temporal discharge data.

4.5 Fraser River dissolved fluxes in global context

It is noteworthy that the effect of runoff in the Fraser basin is to bias the dissolved load towards contributions from older lithologies. Using the same construction as the model described above, an “area-based” prediction of the basin-integrated average bedrock age has the form:

$$BA_{\text{basin}} = \frac{\sum_i (BA_i A_i)}{\sum_i A_i} \quad (3)$$

where BA is the average bedrock age and A is the area of a given subdrainage basin. Since digital bedrock maps are available at reasonably high resolution (1:5,000,000) for this basin (Wheeler et al., 1997), the true average bedrock age of the Fraser basin is well constrained at 260 ± 39 Ma (Peucker-Ehrenbrink et al., 2010). Using only the eight modeled tributaries in Eq. 3, the area-based estimate is very similar: 280 Ma. If the true average bedrock age for the entire basin is assumed to be 260 Ma, then the 24% of the drainage area not included in our model

(62,000 km²) has an average bedrock age of 171 Ma. This supports the conclusion of the ⁸⁷Sr/⁸⁶Sr model, which shows a disproportionate contribution from portions of the basin draining older, more radiogenic lithologies.

The area-based formulation can be modified to use discharge as follows:

$$BA_{\text{basin}} = \frac{\sum_i (BA_i Q_i)}{\sum_i Q_i} \quad (4)$$

where Q_i is the total annual average discharge for an individual tributary (Table 1). Applying Eq. 4 to the eight modeled tributaries predicts a much older basin-integrated average bedrock age of 356 Ma. Hence the runoff regime and weathering rates in the Fraser River have the effect of drawing a disproportionate fraction of dissolved material from subbasins with older bedrock lithologies. This is the opposite offset to what is observed for global exorheic continental runoff, for which the area-average bedrock age is 453 Ma, while the discharge-weighted average age is 394 Ma (Peucker-Ehrenbrink et al., 2010). The headwater regions of the Fraser basin, with bedrock composed mainly of old (>600 Ma) sedimentary rock, are distinct from global average sedimentary rock, which is generally young, 246 ± 42 Ma; while global average volcanic rock is slightly older, 331 ± 52 Ma (Peucker-Ehrenbrink and Miller, 2007). The offset between discharge- and area-weighted bedrock age, both in the Fraser basin and globally, thus appears to reflect the generally higher chemical weathering rate of sedimentary rocks compared to volcanic rocks (Meybeck, 1987; Gaillardet et al., 1999). Given that the headwater regions with the oldest lithologies in the Fraser basin also correspond to the most easily weathered rock types, this portion of the Fraser basin also exerts the dominant control on atmospheric CO₂ consumption by chemical weathering (Amiotte Suchet et al., 2003). The older discharge-weighted bedrock age of the Fraser basin underscores the importance of headwater snowmelt and bedrock distribution

to weathering processes in this river, despite year-round high runoff in regions draining the Coast Range. Large river basins such as the Fraser, which reach inland far past the young lithologies of active margins, have a fundamentally different impact on riverine fluxes to the ocean compared to small mountainous watersheds lining the periphery of active continental margins.

5. Conclusions

The exceptional diversity of bedrock lithology and seasonal hydrology in the Fraser River basin are reflected in the geochemical signatures of its tributaries and their variable admixtures. The basin-wide and time series characterizations of dissolved inorganic species in the Fraser River presented here show that:

- Concentrations of most dissolved elements derive from natural weathering processes, with the exception of Cl and Na, which are sourced largely from sea salt aerosols.
- Isotope tracers of water (δD) and dissolved weathering products ($^{87}\text{Sr}/^{86}\text{Sr}$) serve as source indicators for distinct portions of the drainage basin. The dynamic range of dissolved $^{87}\text{Sr}/^{86}\text{Sr}$ between tributaries allows this tracer to serve as a geochemical fingerprint of specific regions across the basin.
- A mixing model of $^{87}\text{Sr}/^{86}\text{Sr}$ demonstrates that the time series records a seasonal shift in source material. Less radiogenic-dominated runoff (representing the Coast Range tributaries) in fall and winter transitions to substantial radiogenic contributions (deriving from headwater subbasins) in spring and summer.
- The discharge-weighted average bedrock age of the Fraser River is significantly older than the basin area-weighted average, demonstrating the dominance of old sedimentary lithologies to the chemical weathering flux of this basin.

Since the bulk of water, and thus elemental, flux occurs during spring and summer snowmelt, the overall composition of material exported to the ocean by the Fraser River is weighted disproportionately to material derived from the most upstream portions of the drainage basin. This spatial bias has important implications for understanding signals recorded in the chemistry of large rivers and sedimentary deposits influenced by such systems. In modern settings, awareness of the relative importance of different portions of a drainage basin to the overall chemical load is necessary for identifying lithologic and biogeoclimatic zones driving weathering fluxes. Furthermore, when large river-dominated sedimentary records are probed for signs of past changes in weathering activity and terrestrial climate, a deeper knowledge of spatial heterogeneity in weathering across the river basin is critical.

Site	IGSN	Date (yyyy-mm-dd)	Lat (°N)	Lon (°W)	Distance from source (km)	Elevation (masl)	Average precipitation (mm a ⁻¹)	Upstream drainage area (km ²)	Average bedrock age (Ma)	Average discharge (km ³ a ⁻¹)
Fraser at Fitzwilliam	GRO000009	2009-08-03	52.8526	118.6063	50	1,085	594	672	764	1.4
	GRO000027	2010-10-14								
	GRO000073	2011-06-03								
Fraser at McBride	GRO000011	2009-08-04	53.3023	120.1411	230	713	679	6,907	738	6.2
	GRO000030	2010-10-14								
	GRO000070	2011-06-02								
Fraser at Hansard	GRO000012	2009-08-04	54.0817	121.8462	480	604	644	18,088	700	14.5
	GRO000038	2010-10-16								
	GRO000066	2011-06-01								
Fraser at Stoner	GRO000018	2009-08-08	53.6384	122.6652	615	550	641	80,731	345	
	GRO000041	2010-10-19								
Fraser at Lillooet	GRO000022	2009-08-10	50.7080	121.9132	1050	200	330	152,364	254	54.7
	GRO000045	2010-10-21								
	GRO000058	2011-05-28								
Fraser at Lytton	GRO000008	2009-08-01	50.2479	121.5910	1110	145	433	156,342	251	
	GRO000047	2010-10-22								
Fraser at Hope	GRO000048	2010-10-24	49.3893	121.4557	1210	34	2,008	216,561	281	85.6
	GRO000055	2011-05-27								
Fraser at Fort Langley	GRO000001	2009-07-30	49.1801	122.5672	1315	3	1,789	228,776	274	
	GRO000025	2009-08-13								
	GRO000051	2010-10-25								
	GRO000076	2011-06-07								
Fraser at Vancouver	GRO000002	2009-07-28	49.2145	122.7829	1336	1	1,708	228,993	274	99.6
	GRO000052	2010-10-27								
	GRO000075	2011-06-06								
Yellowhead Lake Robson River	GRO000028	2010-10-14	52.8515	118.6027	49	1,086	594	132	768	
	GRO000010	2009-08-03								
	GRO000029	2010-10-14								
	GRO000074	2011-06-03								
Small River	GRO000031	2010-10-15	53.0602	119.6139	185	756	631	252	732	
	GRO000072	2011-06-02								
Holmes River	GRO000032	2010-10-15	53.2518	120.0289	223	725	631	803	752	
	GRO000071	2011-06-02								
Dore River	GRO000033	2010-10-15	53.3221	120.2251	235	725	679	412	770	0.4
	GRO000069	2011-06-02								

Goat River	GRO000034	2010-10-15	53.4946	120.6060	265	717	679	658	770	
	GRO000068	2011-06-02								
Bowron River	GRO000014	2009-08-05	53.8971	121.9869	478	708	601	3,168	530	
	GRO000035	2010-10-15								
	GRO000062	2011-05-31								
McGregor River	GRO000013	2009-08-05	54.2202	121.9020	500	606	601	5,463	672	6.8
	GRO000037	2010-10-16								
	GRO000065	2011-06-01								
Willow River	GRO000015	2009-08-06	54.0678	122.4675	555	582	644	3,157	324	1.1
	GRO000036	2010-10-15								
	GRO000063	2011-05-31								
Nechako River	GRO000016	2009-08-06	53.9265	122.7379	575	570	496	47,148	183	8.8
	GRO000039	2010-10-17								
	GRO000064	2011-05-31								
Blackwater River	GRO000019	2009-08-08	53.2891	123.1380	705	624	511	11,865	49	1.1
	GRO000040	2010-10-18								
	GRO000061	2011-05-30								
Quesnel River	GRO000020	2009-08-09	52.9725	122.4935	770	472	693	12,100	429	7.4
	GRO000042	2010-10-19								
	GRO000060	2011-05-30								
Chilcotin River	GRO000021	2009-08-09	51.8307	122.5718	805	448	338	19,595	61	3.2
	GRO000043	2010-10-20								
	GRO000059	2011-05-29								
Bridge River	GRO000023	2009-08-10	50.7513	121.9339	1,045	208	519	4,748	155	
	GRO000044	2010-10-21								
	GRO000057	2011-05-28								
Thompson River	GRO000007	2009-08-01	50.2367	121.5315	1,111	145	279	55,616	381	24.4
	GRO000046	2010-10-22								
	GRO000056	2011-05-27	50.3461	121.3902						
Harrison River	GRO000006	2009-07-31	49.2361	121.9621	1,265	10	1,755	8,397	151	14.0
	GRO000049	2010-10-24								
	GRO000054	2011-05-26								
Pitt River	GRO000024	2009-08-13	49.3496	122.6162	1,335	5	2,253	1,134	127	
	GRO000050	2010-10-25								
	GRO000053	2011-05-26								

Table 1. Sampling campaigns of the Fraser River main stem and tributaries were carried out in summer 2009 (28 Jul – 13 Aug), fall 2010 (14 – 27 Oct), and spring 2011 (26 May – 7 Jun). International Geo Sample Number (IGSN) codes refer to an open online database of archived metadata (www.geosamples.org). Elevations are shown in meters above sea level (masl). Average precipitation is compiled from Environment Canada National Climate Data and Information Archive records for 1971 – 2000 (climate.weatheroffice.gc.ca) for weather stations corresponding to our sampling sites. Average discharge values for gauged tributaries represent the means for all years of Environment Canada records. These records range from 36 years (Willow River) to 100 years (Fraser at Hope). Site coordinates were determined in the field with a handheld GPS (Garmin, WGS 1984 datum). Note that, in some sources, the Blackwater River is referred to as the West Road River.

Site	IGSN	Flow Stage	NH ₄	SiO ₂	PO ₄	NO ₃ +NO ₂	TA	Ca	Mg	Na	SO ₄	Cl	K	Sr	Ba	Σ ^{ex+} (%)	⁸⁷ Sr/ ⁸⁶ Sr diss.	δD (‰)	δ ¹⁸ O (‰)
Fraser at Fitzwilliam	GRO000027	low	0.41	58	0.11	2.2	813	362	308	34.5	255	6.8	5.75	0.789	0.071	1.9	0.75152	-146.4	-19.14
	GRO000009	med					537	229	211	21.9	176	2.9	4.70	0.547	0.051	0.8	0.75150	-145.1	-19.09
	GRO000073	high	0.14	46	0.19	2.9	679	256	209	30.1	148	8.5	4.17	0.541	0.038	-1.0	0.74884	-155.8	-20.55
Fraser at McBride	GRO000030	low	0.33	31	0.07	2.5	1104	495	205	37.4	208	8.1	15.13	1.606	0.066	-2.5	0.72686	-143.4	-18.77
	GRO000011	med					730	352	114	16.3	110	4.0	10.48	0.955	0.029	0.3	0.72480	-148.8	-19.70
	GRO000070	high	0.33	41	<0.05	8.4	867	462	173	30.8	121	4.8	10.72	1.383	0.049	8.3	0.72738	-153.6	-20.30
Fraser at Hansard	GRO000038	low	0.36	86	<0.05	1.1	1936	697	244	64.9	67	10.8	16.75	1.370	0.205	-2.9	0.71598	-132.2	-17.06
	GRO000012	med					1110	495	156	28.7	116	2.6	12.38	1.236	0.070	-0.1	0.72250	-145.5	-19.20
	GRO000066	high	0.31	51	<0.05	8.4	1033	551	163	31.5	80	4.4	9.21	1.337	0.070	10.2	0.71583	-147.8	-19.54
Fraser at Stoner	GRO000041	low	0.70	40	<0.05	2.9		538	197	140.7	131	28.5	14.04	1.317	0.108		0.71928	-135.3	-17.54
	GRO000018	med					977	410	140	79.0	78	14.1	12.96	0.909	0.083	-1.9	0.71704	-137.3	-17.68
Fraser at Lillooet	GRO000045	low	0.61	84	<0.05	3.3		465	179	148.2	135	22.2	16.05	1.257	0.097		0.71639	-120.7	-12.93
	GRO000022	med						426	137	92.7	86	13.0	15.20	0.998	0.084		0.71496	-137.9	-17.69
	GRO000058	high	0.47	99	0.11	5.9	1040	476	166	96.3	42	12.8	19.85	1.054	0.090	10.3	0.70440	-143.2	-18.61
Fraser at Lytton	GRO000047	low	0.38	48	<0.05	2.8		501	195	157.1	125	19.4	18.08	1.224	0.095		0.71529	-134.8	-17.35
	GRO000008	med					968	425	134	81.9	83	9.0	14.58	0.990	0.086	3.0	0.71530	-138.6	-17.91
Fraser at Hope	GRO000048	low	0.54	55	<0.05	2.9		459	171	144.8	111	22.0	18.83	1.132	0.092		0.71503	-132.9	-17.26
	GRO000055	high	0.30	97	0.15	6.3	755	362	114	91.4	41	20.9	16.80	0.769	0.083	10.5	0.71090	-129.5	-17.12
Fraser at Fort Langley	GRO000051	low	0.93	55	<0.05	5.5	983			102	21.8			1.029	0.090		0.71381	-128.5	-16.51
	GRO000001	med					832	486	147	110.0	78	18.5	21.88	0.897	0.092	16.3	0.71380	-133.7	-17.38
	GRO000076	high	0.29	95	0.13	4.9	849	344	113	80.6	49	15.5	16.92	0.852	0.100	2.5		-136.0	-17.83
Fraser at Vancouver	GRO000052	low	1.10	53	0.43	7.3											0.70467		
	GRO000002	med					693	420	116	94.7	66	15.1	18.74	0.751	0.082	17.2	0.71340	-125.1	-16.45
Yellowhead Lake Robson River	GRO000028	low	0.39	52	0.08	0.9		438	478	49.8	249	15.7	4.96	0.906	0.049		0.74540	-146.4	-18.92
	GRO000029	low	0.30	14	0.11	4.4	1411	535	245	15.9	117	4.6	4.70	2.373	0.159	-2.1	0.71144	-129.3	-14.67
	GRO000010	med					1219	515	183	9.5	71	43.3	3.94	1.834	0.121	0.1	0.71110	-142.4	-17.95
Small River	GRO000074	high	0.18	24	<0.05	6.6	1593	661	318	19.0	108	5.7	5.06	2.757	0.182	4.4	0.71179	-150.8	-20.04
	GRO000031	low	0.35	49	0.07	6.0		634	236	31.9	253	1.9	5.30	1.355	0.029		0.72865	-145.6	-19.15
	GRO000072	high	1.07	41	0.22	10.7		578	176	25.7	122	2.0	5.34	1.079	0.025		0.72877	-138.8	-15.72
Holmes River	GRO000032	low						488	217	48.1	205	5.5	4.80	1.790	0.054		0.73216	-141.5	-18.66
	GRO000071	high	0.32	41	0.05	4.3		374	148	31.4	92	2.5	4.49	1.189	0.031		0.73229	-153.7	-20.23
Dore River	GRO000033	low	0.35	44	0.07	6.8		575	199	29.8	233	1.3	4.43	2.535	0.012		0.73008	-138.5	-18.29
	GRO000069	high	0.44	34	<0.05	14.7		453	129	22.0	90	2.3	4.50	1.733	0.011		0.72960	-143.9	-17.62
Goat River	GRO000034	low	0.34	57	0.07	5.9		704	177	38.6	181	6.8	2.81	2.615	0.022		0.71766	-136.9	-17.82
	GRO000068	high	0.45	45	0.21	10.7		695	139	31.1	81	6.7	2.77	2.224	0.015		0.71620	-142.7	-18.51
Bowron River	GRO000035	low	0.34	69	0.06	<0.05		641	139	34.6	36	3.6	5.39	1.650	0.213		0.71343	-133.8	-17.24
	GRO000014	med					1624	714	160	37.7	33	3.1	5.57	1.608	0.223	2.8	0.71350	-135.7	-17.58
	GRO000062	high	0.46	66	<0.05	2.2	1029	516	101	25.1	14	2.5	5.17	1.204	0.074	8.8	0.71293	-141.3	-18.26
McGregor River	GRO000037	low	0.32	49	0.08	5.0	1647	590	203	26.7	57	4.9	5.57	0.785	0.100	-4.3	0.71999	-129.7	-17.02
	GRO000013	med					1402	566	155	16.4	43	3.0	4.28	0.612	0.075	-0.9	0.71860	-141.1	-18.75
	GRO000065	high	0.27	30	0.22	8.4	1098	507	156	14.2	20	3.1	4.42	0.528	0.057	8.3	0.72161	-148.5	-19.65
Willow River	GRO000036	low	0.23	130	<0.05	<0.05	1019	365	129	56.1	33	9.7	8.02	0.793	0.142	-2.0	0.71434	-110.9	-10.83
	GRO000015	med					1161	443	161	72.2	29	7.9	11.92	0.908	0.152	2.6	0.71340	-133.7	-16.91
	GRO000063	high	0.08	88	0.17	0.4	462	262	86	40.9	13	5.0	9.62	0.500	0.063	20.4	0.70532	-142.8	-18.66

Nechako River	GRO000039	low	0.31	92	0.27	<0.05		349	169	109.3	49	8.5	17.84	0.873	0.130		0.70511	-130.4	-15.94
	GRO000016	med					779	287	113	83.6	34	6.0	13.13	0.644	0.094	2.4	0.70500	-130.0	-15.96
Blackwater River	GRO000064	high	0.06	97	0.11	0.1	819	355	168	140.3	34	10.5	26.46	0.920	0.118	14.9	0.72019	-134.5	-16.49
	GRO000040	low	0.33	295	0.24	2.3	1553	320	291	227.8	15	9.6	50.95	0.748	0.047	-3.0	0.70438	-135.5	-16.50
	GRO000019	med					1738	398	377	257.7	15	7.4	57.95	0.915	0.059	2.5	0.70446	-137.6	-16.75
Quesnel River	GRO000061	high	<0.05	269	0.15	0.8	948	284	242	177.2	10	9.8	52.46	0.615	0.073	13.5	0.71297	-144.7	-18.32
	GRO000042	low					1056	428	97	36.3	80	4.1	8.95	1.555	0.056	-5.4	0.71487	-135.5	-17.53
	GRO000020	med					986	456	93	35.7	73	3.1	9.83	1.533	0.050	0.4	0.71476	-138.0	-17.79
Chilcotin River	GRO000060	high	0.14	52	<0.05	7.4	1093	557	132	49.3	53	16.6	11.77	1.575	0.074	8.4	0.70481	-141.0	-18.31
	GRO000043	low	0.19	78	<0.05	<0.05	710	227	99	103.1	70	7.7	19.35	0.661	0.060	-5.0	0.70426	-138.5	-17.72
	GRO000021	med					525	218	58	66.8	63	4.9	18.10	0.538	0.047	-1.5	0.70416	-138.9	-17.82
Bridge River	GRO000059	high	0.06	228	1.34	0.8	1365	392	349	274.0	48	10.4	55.78	1.010	0.079	10.4	0.71396	-147.0	-18.73
	GRO000044	low	0.47	92	0.06	1.2	1688	428	412	120.8	179	16.5	15.04	1.427	0.098	-6.4	0.70482	-140.6	-18.44
	GRO000023	med					1315	381	350	103.8	132	15.5	16.47	1.094	0.080	-0.4	0.70481	-138.9	-18.24
Thompson River	GRO000057	high	0.36	132	0.08	5.7	516	365	154.0	124	16.2	18.52	1.642	0.082		0.71225	-141.2	-18.61	
	GRO000046	low	0.35	70	0.06	4.1	721	287	81	88.9	94	19.4	20.09	0.853	0.065	-4.7	0.71267	-132.6	-17.17
	GRO000007	med					642	287	68	70.0	71	15.4	19.04	0.801	0.057	0.0	0.71290	-135.6	-17.76
Harrison River	GRO000056	high	0.97	111	0.19	3.7	769	359	119	122.4	64	19.0	26.71	0.929	0.075	9.4	0.70448	-136.2	-17.68
	GRO000049	low	8.19	57	0.18	2.2	371	156	35	54.8	45	13.8	16.66	0.334	0.072	-2.3	0.70437	-113.1	-15.16
	GRO000006	med					306	156	27	55.6	51	15.4	14.89	0.318	0.064	1.3	0.70410	-113.7	-15.39
Pitt River	GRO000054	high	0.51	82	0.22	4.0	304	165	32	59.0	46	11.0	17.62	0.345	0.079	7.3	0.71068	-111.1	-15.11
	GRO000050	low	0.82	11	<0.05	4.3		53	9	28.7	15	9.5	7.12	0.126	0.034		0.70483	-94.5	-13.07
	GRO000024	med						54	9	25.5	19	11.2	7.47	0.131	0.033		0.70465	-98.7	-13.44
	GRO000053	high	1.10	40	0.16	4.9	98	65	11	39.3	16	15.6	6.87	0.143	0.038	15.5	0.70424	-93.9	-13.14
Internal Precision			9.7%	1.5%	11.3%	2.4%	0.2%	2.1%	2.5%	2.6%	0.6%	1.4%	2.6%	2.0%	2.2%		0.000008	0.1	0.03
External Precision				3.5%	6.3%	4.0%	0.03%	3.8%	6.3%	1.9%	0.5%	0.5%	4.3%	2.4%	3.6%		0.000020	0.3	0.02
Accuracy							0.3%	5.2%	4.1%	1.6%			0.8%	1.1%	5.7%		0.000042	1.0	0.07

Table 2. Samples were collected at three flow stages: low (fall 2010), medium (summer 2009), and high/freshet (spring 2011). All dissolved solute concentrations are defined as material passing through a 0.22 μm filter and shown in units of $\mu\text{mol L}^{-1}$. \sum_{ex}^+ is the excess positive charge as a percent of the total ionic charge of major ions. The final rows show the average precision and accuracy of each measurement. Internal precision indicates the average standard deviation of a single measurement; external precision indicates the uncertainty of certified values of international standard reference materials. Accuracy for cation concentrations (Ca, Mg, Na, K, Sr, Ba) indicates the difference between concentrations determined from dilution curves of two different standards: SLRS-5 (National Research Council Canada) and NIST 1640a (U.S. National Institute of Standards and Technology). For total alkalinity (TA), accuracy

indicates the average error given a $2 \mu\text{mol L}^{-1}$ measurement uncertainty. For $^{87}\text{Sr}/^{86}\text{Sr}$, $\delta^{18}\text{O}$, and δD , accuracy indicates the average absolute difference between certified and measured values of standard reference materials.

IGSN	Date (yyyy-mm-dd)	Site	Discharge at Mission ($\text{m}^3 \text{s}^{-1}$)	NH ₄	SiO ₂	PO ₄	NO ₃ + NO ₂	TA	Ca	Mg	Na	SO ₄	Cl	K	Sr	Ba	⁸⁷ Sr/ ⁸⁶ Sr diss.	δD (‰)	$\delta^{18}\text{O}$ (‰)
GRO000001	2009-07-30	FL	4,694					832	486	147	110	78	18.5	21.9	0.897	0.092	0.71380	-133.7	-17.38
GRO000025	2009-08-13	FL	3,416					811	344	101	83	77	16.8	17.6	0.833	0.085	0.71284	-130.4	-17.15
GRO000077	2009-09-17	FL	2,034						382	124	102	90	19.1	19.1	0.893	0.088	0.71340	-128.5	-16.81
GRO000078	2009-10-17	FL	1,410						351	124	117	94	30.6	21.8	0.814	0.094	0.71223	-115.3	-15.21
GRO000079	2009-10-31	NW	1,926						220	81	106	61	45.4	17.6	0.528	0.061	0.71101	-101.9	-13.93
GRO000080	2009-11-29	NW	2,210						199	63	97	50	41.8	15.9	0.465	0.061	0.70929	-97.7	-13.51
GRO000081	2010-01-26	FL	1,338						405	146	156	93	46.6	22.2	0.921	0.104	0.71051	-120.8	-15.80
GRO000082	2010-02-23	FL	1,015						447	183	214	112	50.5	26.8	1.031	0.113	0.71039	-121.2	-15.99
GRO000083	2010-03-09	FL	1,122	2.16	122	0.17	10.0		454	177	195	114	52.0	24.5	1.062	0.114	0.71041	-121.4	-15.78
GRO000084	2010-03-30	FL	1,842	1.16	78	0.27	1.7		419	163	166	93	41.5	24.7	0.968	0.109	0.71090	-121.6	-15.80
GRO000085	2010-04-13	FL	1,474	2.14	118	0.18	6.6		435	167	165	88	42.8	24.0	0.995	0.112	0.71075	-124.3	-16.27
GRO000086	2010-05-07	FL	2,958	0.98	117	0.13	5.3		403	142	120	71	28.4	20.5	0.920	0.096	0.71201	-126.5	-16.42
GRO000087	2010-05-21	FL	5,053	0.76	97	0.08	6.9		349	118	107	63	18.7	18.1	0.806	0.090	0.71125	-126.7	-16.65
GRO000088	2010-05-21	NW	5,053						301	101	99	57	19.9	17.2	0.696	0.081			
GRO000089	2010-05-28	FL	5,089	0.91	99	0.06	7.6		368	113	90	64	16.0	17.5	0.855	0.085	0.71284	-131.1	-17.06
GRO000090	2010-06-04	FL	5,769	0.37	94	0.07	5.3		327	99	80	59	15.4	16.6	0.760	0.079	0.71167	-125.6	-16.12
GRO000091	2010-06-04	NW	5,769	0.82	88	0.09	6.3		301	95	82	57	17.7	16.0	0.699	0.075		-123.4	-16.25
GRO000092	2010-06-11	FL	6,143	0.28	92	0.05	1.9		307	86	67	53	11.0	13.5	0.747	0.076	0.71219	-129.1	-17.01
GRO000093	2010-06-11	NW	6,143	0.93	92	0.08	5.8		302	91	82	59	16.8	16.1	0.730	0.074		-125.2	-16.57
GRO000094	2010-06-18	FL	6,583	0.32	84	0.06	1.7		335	101	73	66	10.5	14.9	0.794	0.077	0.71268	-130.2	-17.05
GRO000095	2010-06-18	NW	6,583	0.41	84	0.06	3.7		314	97	75	58	10.8	15.7	0.756	0.076		-128.5	-16.84
GRO000097	2010-07-09	FL	5,491	0.44	84	0.06	2.4		327	95	105	70	31.1	35.4	0.805	0.080	0.71287	-122.8	-15.06
GRO000098	2010-07-09	NW	5,491	0.88	55	0.10	1.8		252	72	65	59	13.9	13.4	0.628	0.068		-122.3	-16.08
GRO000099	2010-07-14	FL	5,670	0.28	62	0.03	1.0		307	89	68	71	10.9	15.5	0.773	0.075	0.71271	-128.6	-16.71
GRO000100	2010-07-20	FL	4,700	0.29	82	0.04	2.7		310	91	70	76	12.5	15.9	0.776	0.077	0.71299	-129.6	-16.85
GRO000101	2010-07-26	FL	4,341	0.31	60	0.05	0.4		321	102	81	80	15.2	19.2	0.807	0.081	0.71284	-129.5	-16.69
GRO000102	2010-07-30	NW	4,153	0.48	55	<0.05	1.6		299	86	72	68	21.5	15.1	0.738	0.075	0.71287	-127.5	-16.73
GRO000103	2010-08-06	FL	3,797	0.18	75	0.05	1.1		317	98	83	79	13.9	19.4	0.784	0.079	0.71291	-130.7	-17.03
GRO000104	2010-08-13	FL	3,475	0.68	64	0.05	1.0		335	104	88	82	19.2	18.4	0.828	0.082	0.71286	-121.9	-14.60
GRO000105	2010-08-20	NW	3,107						263	76	72	60	8.5	14.2	0.643	0.070	0.71251	-122.0	-16.39
GRO000106	2010-08-27	FL	2,477	0.60	65	0.24	5.7		336	99	87	79	9.0	17.1	0.833	0.082	0.71340		
GRO000107	2010-09-11	NW	2,166						273	82	71	58	9.9	11.2	0.663	0.072	0.71343	-127.5	-16.95
GRO000108	2010-09-13	FL	2,068	0.59	47	<0.05	0.9		393	127	102	90	24.2	18.8	0.938	0.089	0.71377	-129.5	-17.08
GRO000109	2010-09-27	FL	2,402	1.48	67	0.12	5.5		372	126	113	91	17.9	21.5	0.914	0.091	0.71286	-125.6	-16.31
GRO000110	2010-10-18	FL	2,047	0.97	71	0.09	3.8		387	131	115	95	18.3	19.5	0.936	0.087	0.71353		
GRO000111	2010-10-21	NW	1,822	1.60	70	0.15	5.0		328	101	91	73	12.8	15.0	0.794	0.080	0.71380	-122.8	-16.19
GRO000051	2010-10-25	FL	2,189	0.93	55	<0.05	5.5	983				102	21.8		1.029	0.090	0.71381	-128.5	-16.51
GRO000112	2010-11-01	FL	1,949	2.37	88	0.20	7.1		399	136	115	88	28.9	19.8	0.938	0.091	0.71319	-124.2	-16.02
GRO000113	2010-11-04	NW	1,875	1.35	51	0.08	7.1		250	82	95	56	23.3	16.5	0.589	0.070	0.71203	-108.1	-14.47
GRO000114	2010-11-15	FL	1,865	2.19	85	0.24	5.8		392	135	122	88	23.4	19.9	0.923	0.093	0.71261		
GRO000115	2010-12-09	FL	1,310	2.37	88	0.20	7.1		423	157	161	97	45.2	23.6	1.003	0.104	0.71150	-121.5	-15.74
GRO000116	2010-12-16	FL	1,423	2.19	85	0.24	5.8		347	124	128	84	32.0	24.0	0.828	0.099	0.71041		
GRO000117	2011-01-11	NW	983	7.31	25	0.30	13.6		458	592	4761	301	4536	120.7	1.663	0.110	0.70978	-111.4	-15.07
GRO000118	2011-01-20	FL	1,258	2.94	58	<0.05	12.6		295	101	120	71	48.5	21.4	0.700	0.091	0.70870	-110.1	-14.74

GRO000119	2011-01-24	NW	1,214	2.86	34	<0.05	8.3	244	84	159	57	98.1	18.1	0.586	0.076	0.70888	-103.9	-14.18	
GRO000121	2011-02-03	FL	1,150	2.62	104	0.24	10.3	413	150	179	100	39.0	22.7	0.969	0.107	0.71023	-119.4	-15.62	
GRO000122	2011-02-08	NW	1,256	2.22	84	0.17	15.6	286	102	149	67	77.9	18.0	0.686	0.085	0.71028	-107.5	-14.51	
GRO000123	2011-02-24	FL	1,022	3.21	99	0.17	9.4	418	150	175	99	52.1	22.7	0.983	0.111	0.71023	-120.7	-15.85	
GRO000124	2011-03-03	FL	903					447	174	208	107	82.2	23.6	1.073	0.124	0.71036	-121.5	-15.66	
GRO000125	2011-03-04	NW	883	3.68	102	0.20	13.0	392	149	273	94	176.9	21.1	0.936	0.111	0.71035	-114.7	-14.77	
GRO000126	2011-03-25	NW	1,039	4.74	94	0.20	9.2	371	135	214	92	131.2	21.8	0.904	0.107	0.70984	-117.0	-15.43	
GRO000127	2011-04-19	FL	1,601	1.83	105	0.26	8.6	440	168	176	88	43.7	25.4	1.036	0.126	0.71040	-127.8	-16.84	
GRO000128	2011-04-21	FL	1,562					413	167	167	86	60.5	24.6	0.986	0.120	0.71042	-129.2	-16.87	
GRO000129	2011-05-03	FL	2,535								68	50.7				0.71064	-134.0	-17.51	
GRO000130	2011-05-10	FL	3,929	2.96	102	0.24	2.5	385	149	148	53	65.7	40.9	0.882	0.122	0.71056	-136.4	-17.70	
GRO000131	2011-05-13	NW	4,888	1.22	97	0.20	5.6	307	108	99	42	40.8	17.7	0.707	0.090	0.71040	-127.0	-16.65	
GRO000132	2011-05-20	FL	7,819	0.56	103	0.16	4.2	402	140	102	50	14.4	20.6	0.913	0.110	0.71123	-130.1	-15.94	
GRO000133	2011-05-25	FL	8,590	<0.05	103	0.18	1.1	913	389	127	97	50	21.0	18.7	0.869	0.101	0.71144	-134.9	-17.52
GRO000134	2011-05-28	FL	9,461														-135.6	-17.78	
GRO000135	2011-06-03	FL	9,904	0.19	90	0.19	1.8	369	122	87	49	17.1	18.8	0.869	0.094	0.71180	-137.3	-17.98	
GRO000076	2011-06-07	FL	10,469	0.29	95	0.13	4.9	849	344	113	81	49	15.5	16.9	0.852	0.100	-136.0	-17.83	
GRO000136	2011-06-10	NW	10,780	0.75	92	0.20	5.1	326	102	78	48	28.2	15.6	0.779	0.085	0.71141	-131.3	-17.17	
GRO000137	2011-06-17	FL	10,010	0.44	84	0.05	5.3	349	106	75	54	14.6	15.7	0.838	0.086	0.71223	-133.1	-16.91	
GRO000140	2011-06-28	FL	10,020	0.99	74	0.07	4.2	795	357	115	78	56	14.0	16.8	0.856	0.081	0.71264	-137.9	-18.02
GRO000141	2011-06-30	FL	9,780	0.15	85	0.22	4.6	327	99	68	54	14.3	14.2	0.804	0.080	0.71234	-135.6	-17.78	
GRO000142	2011-07-08	FL	9,680	0.61	72	0.06	3.8	771	358	108	73	53	12.7	16.3	0.838	0.078	0.71265	-136.6	-17.95
GRO000143	2011-07-15	FL	9,750	0.73	70	0.07	3.7	878	370	112	66	51	12.6	15.8	0.872	0.085	0.71296	-138.2	-18.11
GRO000144	2011-07-19	FL	9,650	0.51	74	0.08	3.1	840	370	118	75	55	13.0	16.0	0.876	0.085	0.71295	-137.1	-18.04
GRO000145	2011-07-29	FL	7,520	0.96	79	0.09	3.3	359	120	83	56	14.8	17.3	0.865	0.090	0.71244	-135.1	-17.72	
GRO000146	2011-08-05	NW	7,154	0.91	56	0.11	0.2	345	112	79	52	15.5	16.2	0.814	0.084	0.71243	-132.4	-17.45	
GRO000147	2011-08-12	FL	5,291	0.35	76	0.09	3.1	366	122	89	63	15.8	17.5	0.883	0.091	0.71243	-134.2	-17.53	
GRO000148	2011-08-16	FL	4,636	1.20	71	0.09	0.9	373	123	94	66	19.3	18.1	0.895	0.092	0.71232	-133.6	-17.46	
GRO000149	2011-08-19	NW	4,264	0.35	67	0.09	1.5	315	105	88	56	19.9	17.0	0.757	0.083	0.71211	-128.0	-16.72	
GRO000150	2011-08-26	FL	4,521	0.68	73	0.10	2.2	381	127	110	70	15.0	20.8	0.910	0.094	0.71229	-133.5	-17.41	
GRO000152	2011-09-08	FL	2,855	2.20	67	0.08	1.2	412	138	101	76	18.9	19.0	0.975	0.100	0.71285	-102.8	-8.27	
GRO000153	2011-09-13	FL	2,657	0.88	74	0.06	2.8	418	143	108	81	21.1	19.8	0.993	0.102	0.71268	-132.0	-17.19	
GRO000154	2011-09-19	FL	2,406	1.42	68	0.08	1.2	415	144	116	81	27.4	20.3	0.986	0.101	0.71278	-131.9	-17.23	
GRO000155	2011-09-26	FL	3,145	1.88	71	0.07	3.3	391	135	108	81	21.8	19.7	0.925	0.095	0.71243			
GRO000156	2011-10-14	FL	2,714	1.97	69	0.12	5.0	783	355	123	105	70	21.8	18.6	0.834	0.084	0.71232	-124.5	-16.42
GRO000157	2011-10-25	FL	2,255	1.40	60	0.11	1.4	893	395	143	124	75	26.2	19.3	0.923	0.093	0.71211	-127.5	-16.55
GRO000158	2011-10-26	FL	2,236	2.04	77	0.11	4.7	864	385	143	124	73	25.1	19.0	0.900	0.093	0.71218	-127.8	-16.75
GRO000159	2011-10-31	FL	2,156					900	398	147	124	74	27.5	20.1	0.923	0.091	0.71239	-128.3	-16.78

Table 3. Time series measurements of concentrations of dissolved nutrients and major and trace element concentrations (all values in $\mu\text{mol L}^{-1}$), and radiogenic Sr and stable H_2O isotope compositions, show seasonal trends in sources of dissolved material in the Fraser basin. Site abbreviations are FL for Fort Langley (see Table 1) and NW for New Westminster (49.2178 °N, -122.8923 °W), two

nearby cities close to the mouth of the Fraser River. Discharge at Mission, the total water flux of the Fraser River, is calculated as the sum of discharge for the Fraser at Hope and the Harrison River. This record was used to calculate annual loads and discharge-weighted average concentrations (Table 4).

	Fraser Flux (mol a ⁻¹)	Discharge-Weighted Average Fraser Concentration (μmol L ⁻¹)	Fraser Literature Concentrations (μmol L ⁻¹)	Ref.	World Average River Concentration (μmol L ⁻¹)	Ref.
HCO ₃	82 ± 13 × 10 ⁹	851 ± 74	1016	1	957	5
			1145	2	852	8
			983	3		
			841	4		
			1000	4		
Ca	35 ± 8 × 10 ⁹	365 ± 27	434	1	374	5
			470	2	367	7
			399	3	334	8
			442	4	470	9
			494	5		
Mg	12.0 ± 2.9 × 10 ⁹	123 ± 13	139	1	169	5
			170	2	152	7
			118	3	138	8
			148	4	193	9
			185	5		
Na	10.5 ± 1.8 × 10 ⁹	110 ± 12	133	1	274	5
			161	2	313	7
			68	3	224	8
			126	4	270	9
			57.8	1	218	5
SiO ₂	8.2 ± 2.0 × 10 ⁹	81.23 ± 0.12	87.4	2	402	6
			81.6	3	173	8
			90.9	4		
			121	5		
			71.4	6		
SO ₄	6.6 ± 0.7 × 10 ⁹	69 ± 6	88.2	1	117	5
			113	2	85.9	8
			83.3	3	190	9
			85.4	4		
			104	5		
Cl	2.8 ± 0.6 × 10 ⁹	29 ± 6	67.7	1	220	5
			44.7	2	162	8
			1.9	3	190	9
			67.7	4		
			42.3	5		
K	1.9 ± 0.3 × 10 ⁹	19.5 ± 1.7	18.4	1	58.8	5
			20.7	2	35.8	7
			18.8	3	33.2	8
			17.9	4	38.0	9
			1.45	1	16.1	5
NO ₃ + NO ₂	0.48 ± 0.09 × 10 ⁹	4.76 ± 0.28	6.29	2	43.0	6
			3.23	3		
			7.07	4		
			14.3	6		
NH ₄	0.12 ± 0.05 × 10 ⁹	1.12 ± 0.19				
Sr	83 ± 19 × 10 ⁶	0.85 ± 0.04	1.14	1	0.68	7
			1.10	2	0.70	9
			0.28	3	1.26	10
PO ₄	13 ± 5 × 10 ⁶	0.125 ± 0.016	1.61	4	1.39	6
			0.25	6		
Ba	8.7 ± 2.1 × 10 ⁶	90 ± 4 × 10 ⁻³	100 × 10 ⁻³	2	167 × 10 ⁻³	7
			134 × 10 ⁻³	3	180 × 10 ⁻³	9

Table 4. Elemental fluxes and discharge-weighted average concentrations for the Fraser River (first two columns) were calculated from time series measurements and Environment Canada discharge data at Mission using LoadEst (Runkel et al., 2004). Uncertainties for these estimates represent 1 s.d. for the average of three annual load estimates (2009, 2010, 2011; see text section 3.1). Numbered references are: (1) Cameron (1996); (2) Cameron et al. (1995); (3) Durum (1960); (4) Meybeck and Ragu (2012); (5) Livingstone (1963); (6) Mayorga et al. (2010); (7) Gaillardet et al. (2003); (8) Meybeck (1979); (9) Miller et al. (2011); and (10) Peucker-Ehrenbrink et al. (2010). For discussion of comparisons, see text sections 4.1 and 4.3.

Reference	Sample Collection Date	Sampling Location	dissolved $^{87}\text{Sr}/^{86}\text{Sr}$
Wadleigh et al. (1985)	May 1979	not reported	0.71195
Cameron and Hattori (1997)	July 1993	Fraser at Vancouver	0.712707 ± 0.000008
Allègre et al. (2010)	not reported	not reported	0.7188
This study	discharge-weighted average	Fraser at Fort Langley	0.7120 ± 0.0003

Table 5. The dissolved $^{87}\text{Sr}/^{86}\text{Sr}$ composition of the Fraser River reported in the literature varies according to which portion of the hydrograph was sampled. The value reported by Allègre et al. (2010) likely represents only the upper third of the Fraser basin. The uncertainty shown for the value of Cameron and Hattori (1997) represents a 2σ analytical error, while the uncertainty given for our discharge-weighted average (2 s.d.) reflects a combination of LoadEst model calibration error and interannual variability.

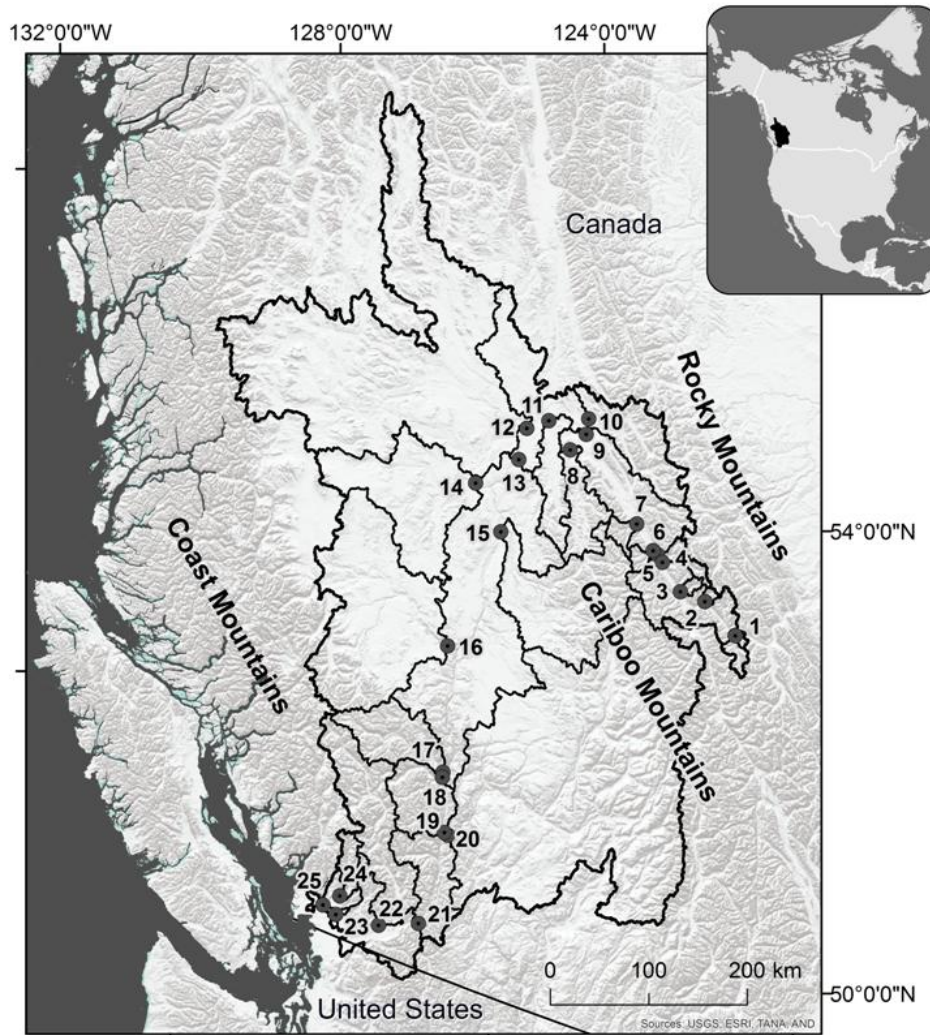


Figure 1. Topographic map of the Fraser River basin with large tributary subdrainage basins outlined. Sampling points are indicated by numbered circles: (1) Fraser at Fitzwilliam; (2) Robson River; (3) Small River; (4) Holmes River; (5) Fraser at McBride; (6) Dore River; (7) Goat River; (8) Bowron River; (9) Fraser at Hansard; (10) McGregor River; (11) Willow River; (12) Nechako River; (13) Fraser at Stoner; (14) Blackwater (West Road) River; (15) Quesnel River; (16) Chilcotin River; (17) Bridge River; (18) Fraser at Lillooet; (19) Fraser at Lytton; (20) Thompson River; (21) Fraser at Hope; (22) Harrison River; (23) Fraser at Fort Langley; (24) Pitt River; (25) Fraser at Vancouver. The Fraser at Mission lies between (22) and (23).

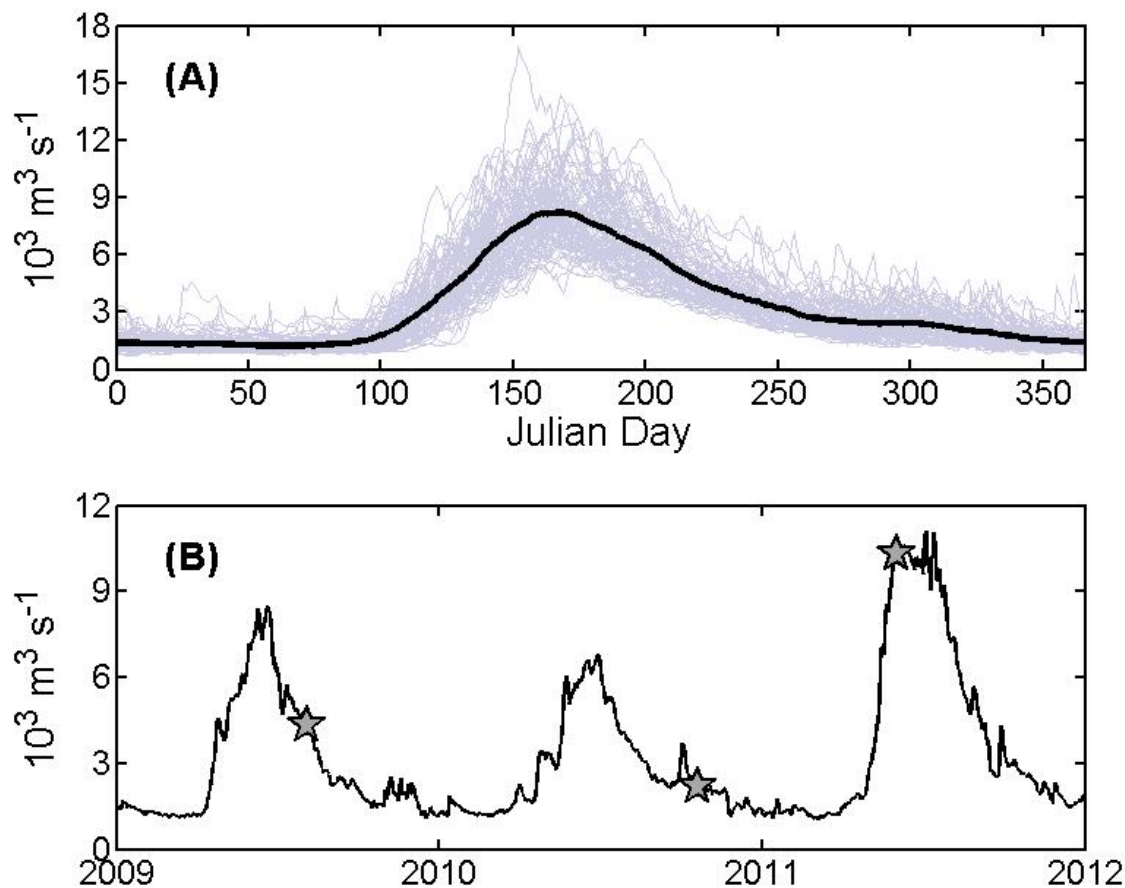


Figure 2. (A) The total Fraser River hydrograph at Mission is characterized by a spring freshet of $\sim 8000 \text{ m}^3 \text{ s}^{-1}$ and winter base flow of $\sim 1800 \text{ m}^3 \text{ s}^{-1}$. Faint curves show individual hydrographs, whereas the bold curve is the average hydrograph for the period of record (1912 – 2011). (B) The recent hydrograph of the Fraser River at Mission shows the variability in the progression and magnitude of the spring freshet from one year to the next. Stars indicate the timing of basin-wide sampling campaigns in this study.

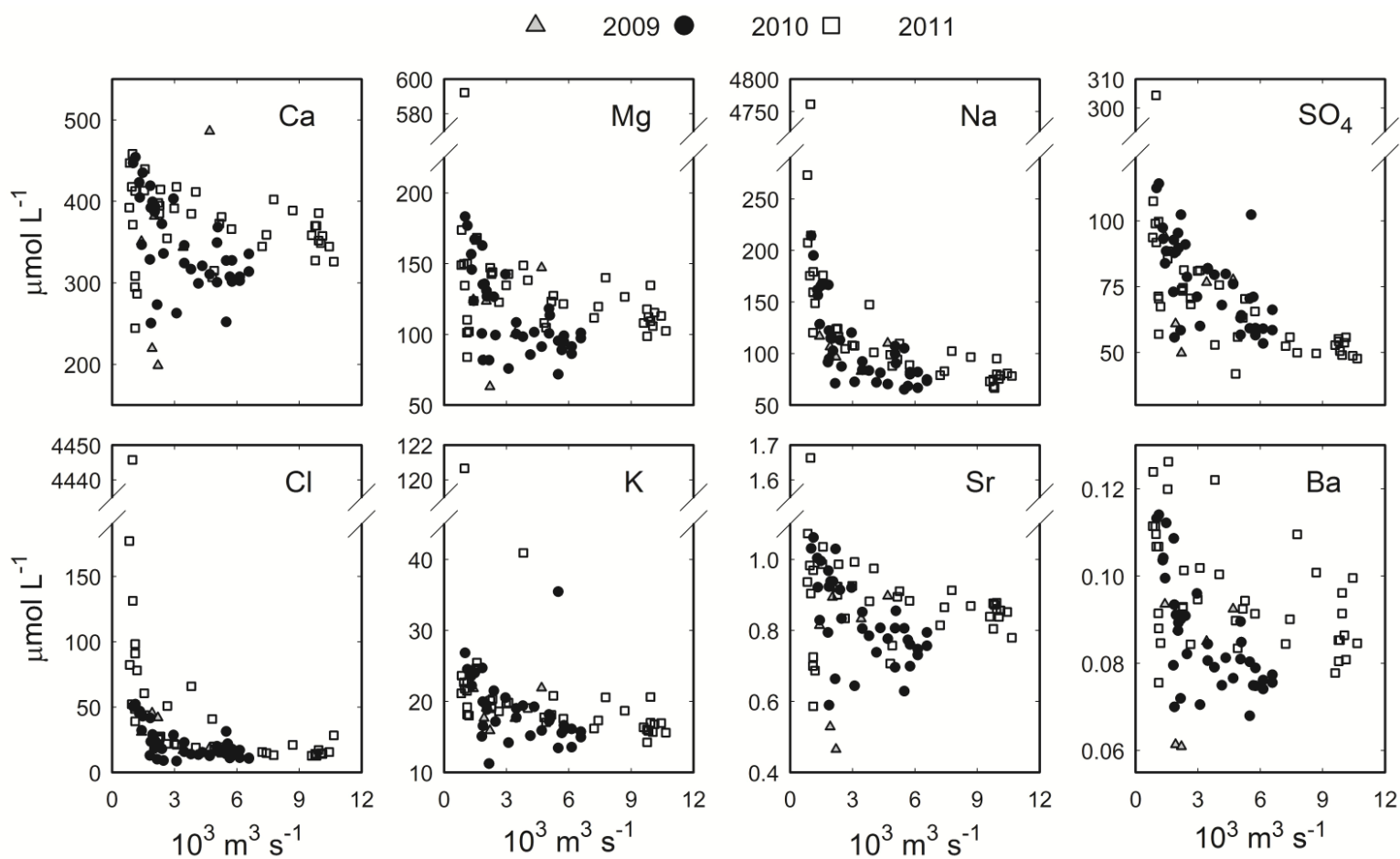


Figure 3. Plots of dissolved element concentrations versus total Fraser River discharge (at Mission) on the day of sampling generally show kinetic-limited chemical weathering behavior with modest dilution when discharge exceeds base flow ($\sim 1800 \text{ m}^3 \text{ s}^{-1}$). The most extreme variability is seen in species strongly affected by sea salt aerosols (Cl, Na).

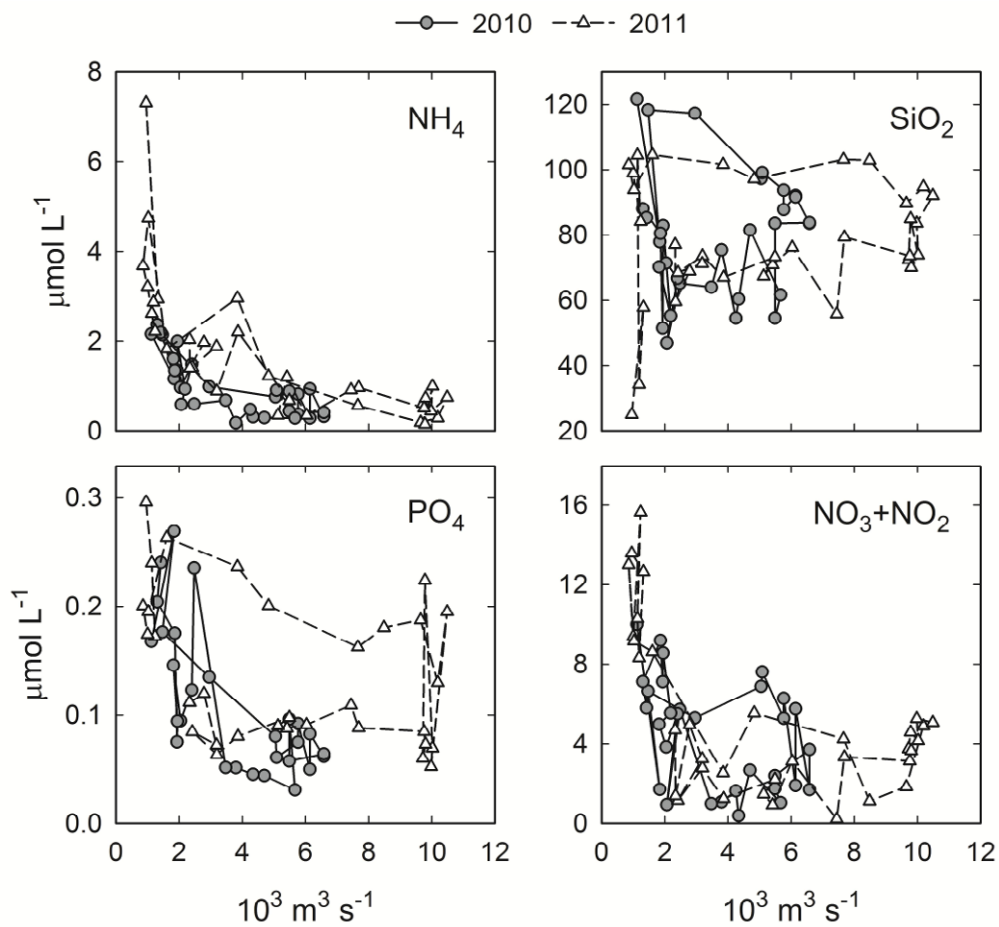


Figure 4. The time series records of inorganic nutrient concentrations exhibit hysteresis behavior (generally counterclockwise) with respect to discharge.

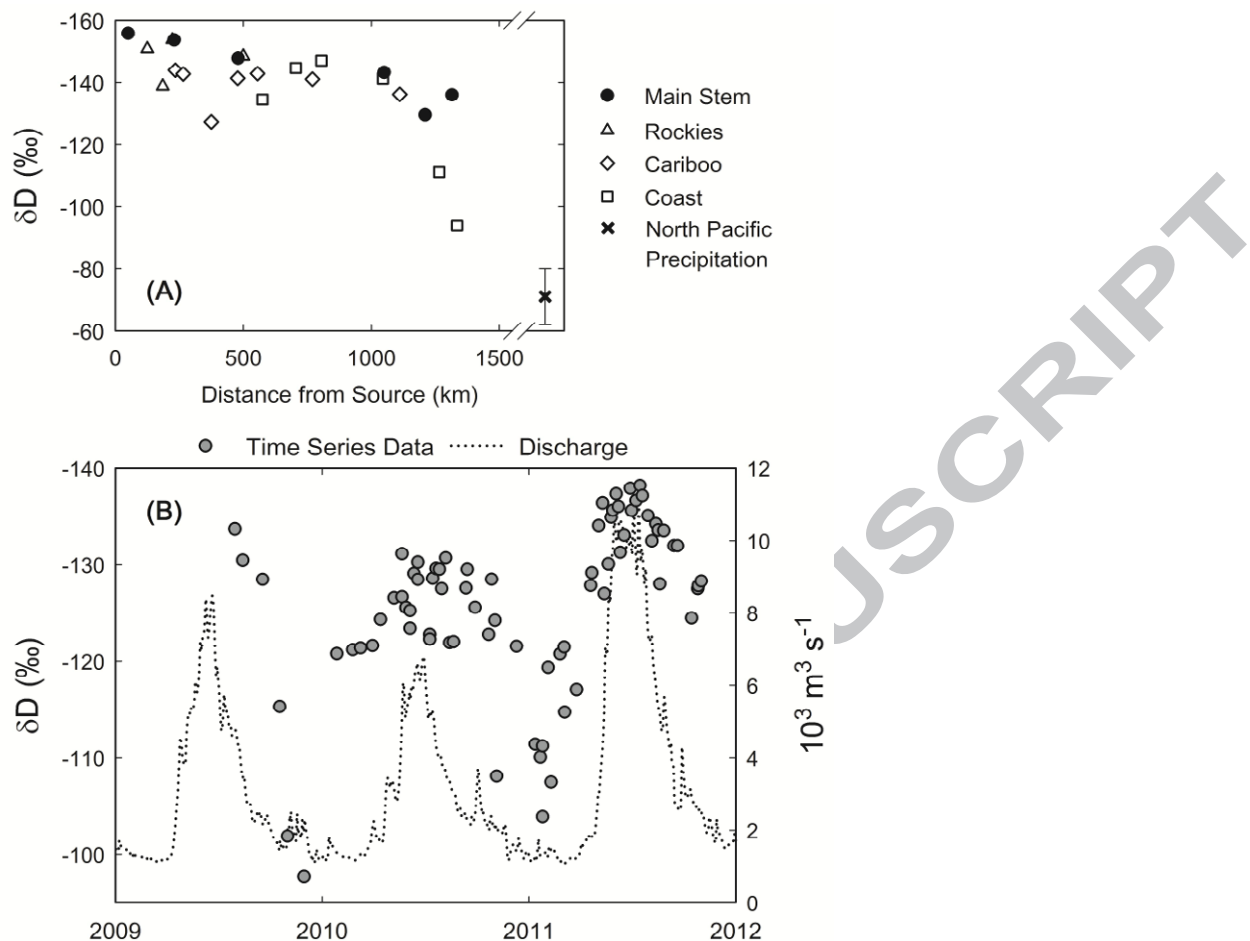


Figure 5. (A) The δD value of precipitation in the Fraser River basin decreases as Pacific Ocean air masses travel inland (right to left on x-axis). In this June 2011 transect, points represent main stem sites, as well as tributaries draining the Rocky Mountain headwaters, the Cariboo Range of the central basin, and the Coast Range of the western basin. The δD composition of precipitation near the Fraser mouth is also shown (error bars indicate ± 1 s.d. of seven years of monthly sampling). (B) The basin-integrated δD composition of the Fraser River shows significant seasonal variability, with more negative spring and summer values indicating greater contributions from snowmelt in the headwaters.

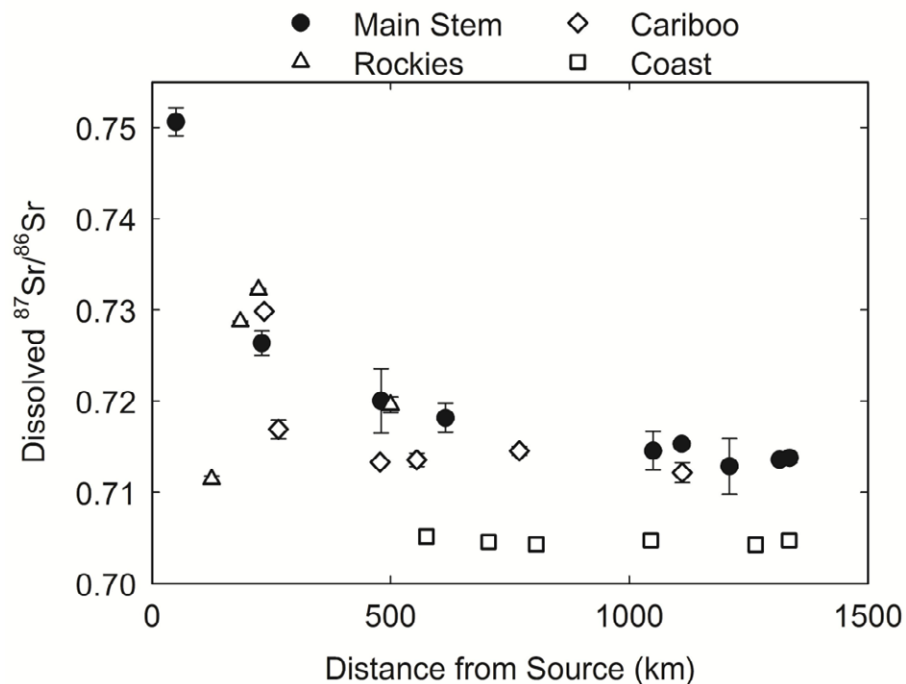


Figure 6. A downstream transect of dissolved $^{87}\text{Sr}/^{86}\text{Sr}$ in the Fraser River shows the abrupt transition between more radiogenic tributary basins in the Rocky and Cariboo Mountains to less radiogenic tributaries draining the Coast Range. Error bars indicate one standard deviation from the average of the three sampling campaigns. Our values for samples collected in summer 2009 (medium flow) are indistinguishable from those reported by Cameron and Hattori (1997) for samples collected in July 1993.

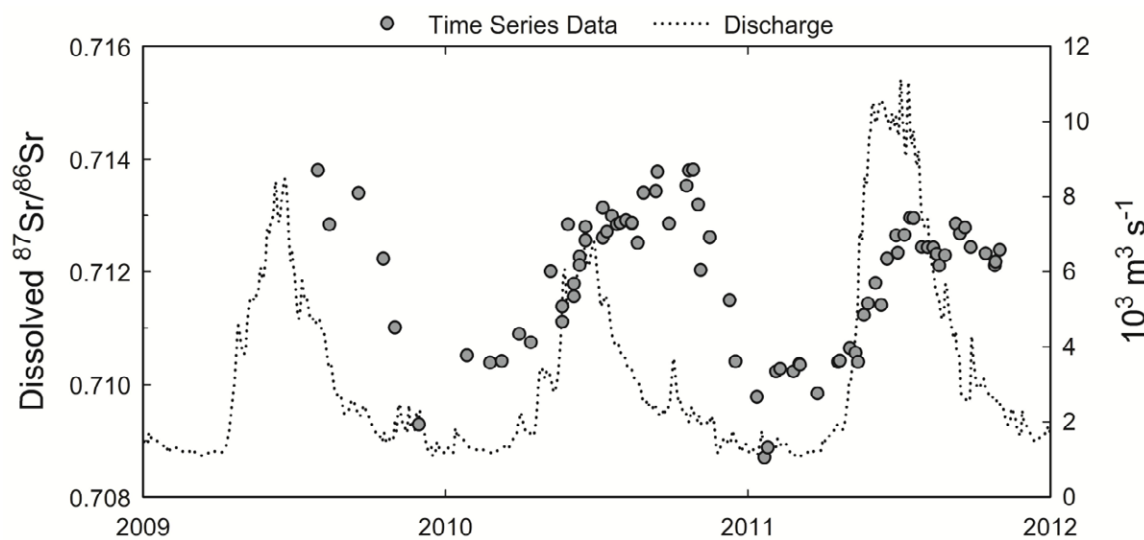


Figure 7. A time series record of dissolved $^{87}\text{Sr}/^{86}\text{Sr}$ in the Fraser River shows a seasonal shift in contributions to the dissolved load from more radiogenic portions of the drainage basin (stronger in spring and summer) to less radiogenic portions (stronger in fall and winter).

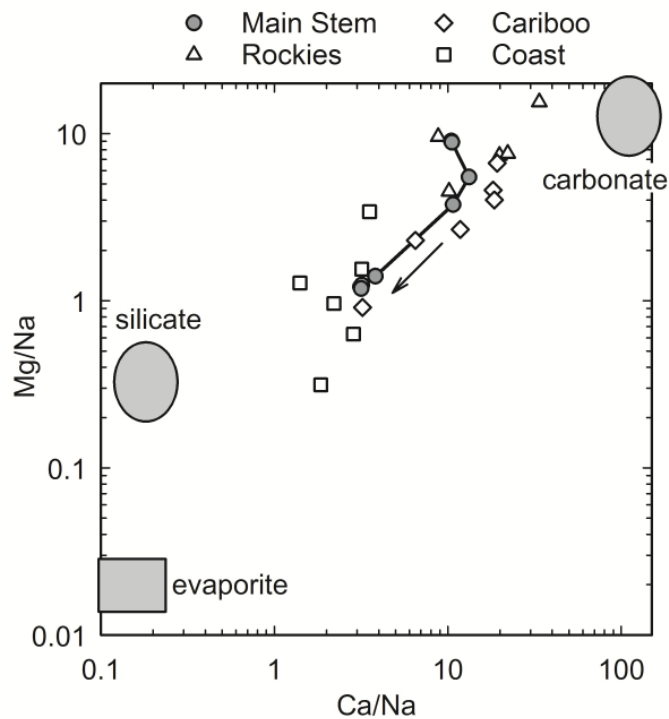


Figure 8. Major element ratios (mol mol^{-1}) of the Fraser River dissolved load indicate a dilution of carbonate-dominated weathering products by material bearing a silicate weathering signature moving downstream (data shown from fall 2010 samples). Main stem sites are connected with a line, and an arrow indicates the direction from headwaters to the delta. Large shapes show the compositions of endmembers for waters draining pure lithologies (Gaillardet et al., 1999).

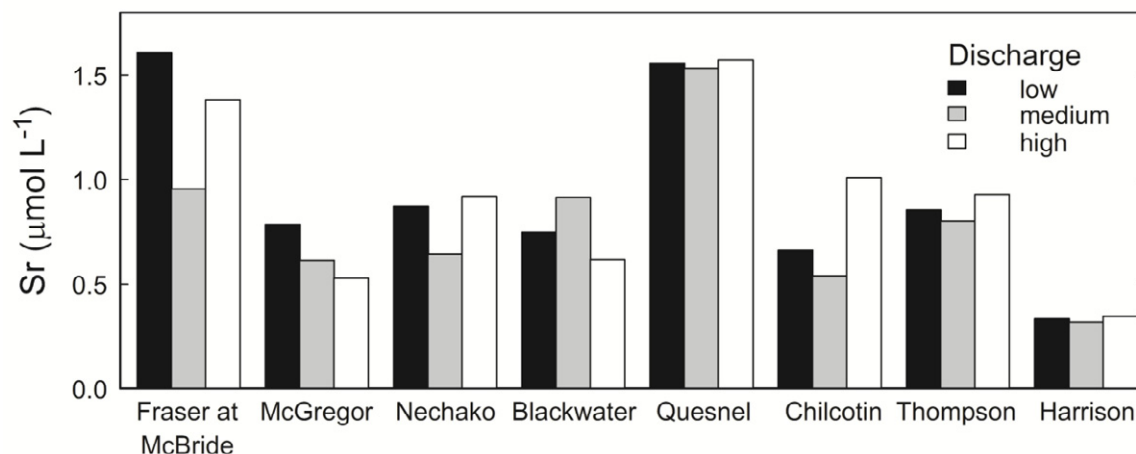


Figure 9. Tributaries included in the $^{87}\text{Sr}/^{86}\text{Sr}$ model do not show a systematic dilution of strontium concentration with discharge conditions at the time of sampling (low in fall 2010, medium in summer 2009, high in spring 2011). In the model, we chose to use average concentrations for each tributary.

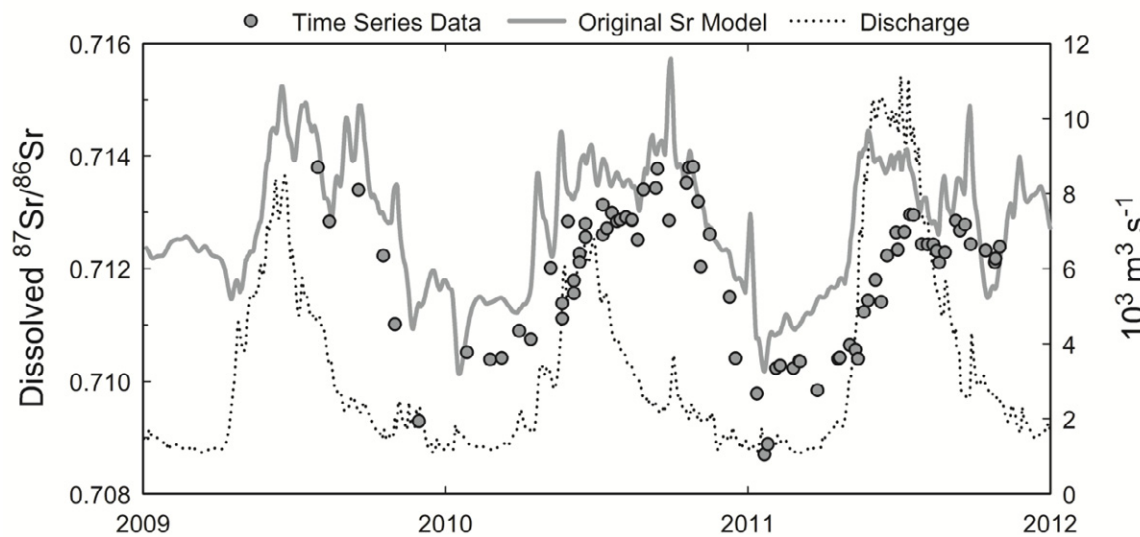


Figure 10. A model of the variability in basin-integrated $^{87}\text{Sr}/^{86}\text{Sr}$ using Sr flux and $^{87}\text{Sr}/^{86}\text{Sr}$ composition of eight subdrainage basins follows the seasonal pattern of the measured time series values.

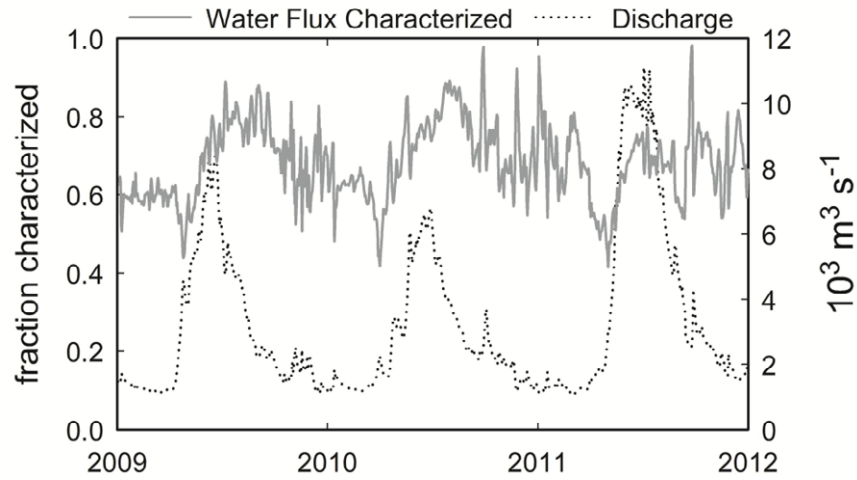


Figure 11. The fraction of total discharge characterized by the original $^{87}\text{Sr}/^{86}\text{Sr}$ model shows that the model characterizes a greater portion of the discharge during spring and summer.

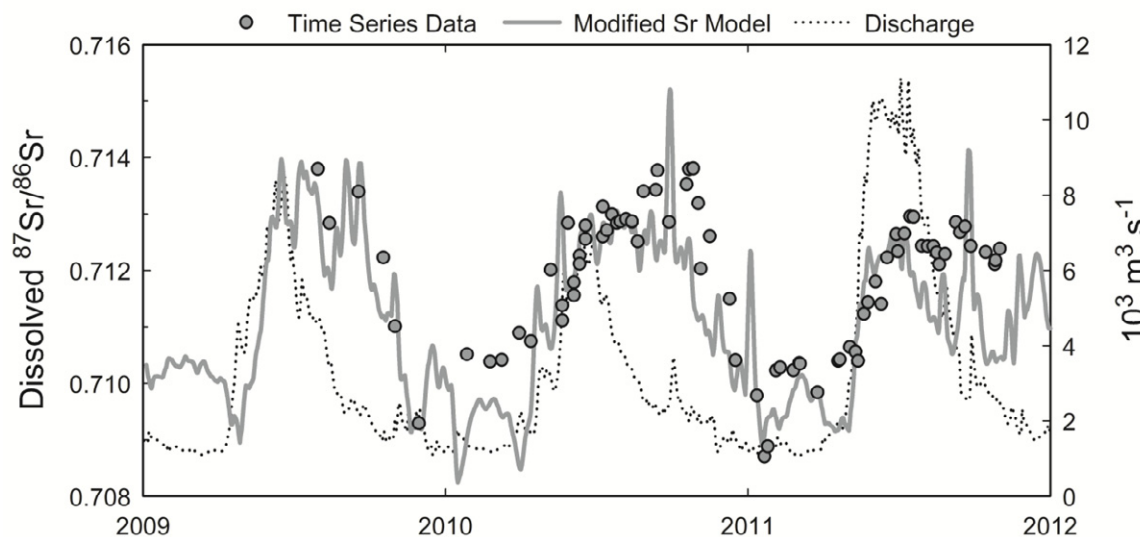


Figure 12. Addition of an unradiogenic ($^{87}\text{Sr}/^{86}\text{Sr} = 0.7046$) component with low Sr concentration ($0.45 \mu\text{mol L}^{-1}$) to the $^{87}\text{Sr}/^{86}\text{Sr}$ model appears to resolve most of the offset between the original model and measured time series values, suggesting that the majority of the uncharacterized flux derives from basins draining the Coast Range.

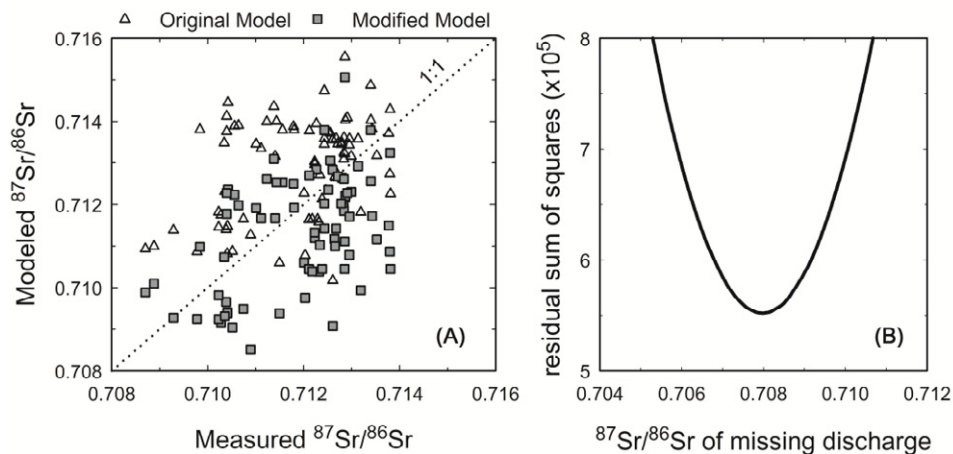


Figure 13. (A) Modeled $^{87}\text{Sr}/^{86}\text{Sr}$ for the original model exhibits, on average, a radiogenic bias when compared to time series measurements on the same day. The modified model with a Coast Range-like composition applied to uncharacterized discharge has, on average, a less radiogenic bias of similar magnitude. (B) Adjusting the $^{87}\text{Sr}/^{86}\text{Sr}$ composition of the uncharacterized discharge to 0.7080 minimizes the residual sum of squares between the time series measurements and the modified model.

Acknowledgements

We thank Scot Birdwhistell and Jerzy Blusztajn (ICPMS Facility), Sean Sylva (Jeffrey Seewald's IC lab), and Paul Henderson (Nutrient Facility) for analytical assistance at WHOI. Liz Drenkard, Meagan Gonnee, and Jill McDermott at WHOI assisted with manipulation and visualization of data. Special thanks to Amber Campbell and Lynne Campo at Environment Canada for providing rating curve information for the Harrison River. We also thank captains Steve Davis, Felix Rohraff, and Wayne Leslie, and mates Norbert Simon, Asar (Jeffrey) Tengku, and Kathy McDonald, of the *Port Fraser*, and Nellie François at Metro Port Vancouver, who facilitated sampling in the delta. MIT/WHOI Joint Program students Katherine Kirsch and Sarah Rosengard assisted with sampling. John Brinckerhoff at WHOI and Pauleen Nuite, Ken Humbke, and Andrew Gray at UFV provided critical support with shipments of gear and samples. Emilio Mayorga generously provided the Global NEWS 2 dataset. Thoughtful comments from Albert Galy and two anonymous reviewers greatly improved this manuscript. This work was supported by the WHOI Academic Programs Office and MIT PAOC Houghton Fund to BMV, a WHOI Arctic Research Initiative grant to ZAW, NSF-ETBC grant OCE-0851015 to BPE and TIE, and NSF grant EAR-1226818 to BPE.

References

- Allègre C. J., Louvat P., Gaillardet J., Meynadier L., Rad S., and Capmas F. (2010) The fundamental role of island arc weathering in the oceanic Sr isotope budget. *Earth Planet. Sci. Lett.* **292**, 51-56. doi:10.1016/j.epsl.2010.01.019.
- Alvarez-Cobelas M., Sánchez-Carrillo S., Angeler D. G., and Sánchez-Andrés R. (2009) Phosphorus export from catchments: a global view. *J. N. Am. Benthol. Soc.* **28**, 805-820. doi:10.1899/09-073.1.
- Amiotte Suchet P., Probst J.-L., and Ludwig W. (2003) Worldwide distribution of continental rock lithology: Implications for the atmospheric/soil CO₂ uptake by continental weathering and alkalinity river transport to the oceans. *Global Biogeochem. Cycles* **17**. doi:10.1029/2002gb001891.
- Armstrong R. L. (1988) Mesozoic and early Cenozoic magmatic evolution of the Canadian Cordillera. *Geol. Soc. Am. Spec. Pap.* **218**, 55-92. doi:10.1130/SPE218-p55.
- Bagard M.-L., Chabaux F., Pokrovsky O. S., Viers J., Prokushkin A. S., Stille P., Rihs S., Schmitt A.-D., and Dupré B. (2011) Seasonal variability of element fluxes in two Central Siberian rivers draining high latitude permafrost dominated areas. *Geochim. Cosmochim. Acta* **75**, 3335-3357. doi:10.1016/j.gca.2011.03.024.
- Bataille C. P. and Bowen G. J. (2012) Mapping ⁸⁷Sr/⁸⁶Sr variations in bedrock and water for large scale provenance studies. *Chem. Geol.* **304-305**, 39-52. doi:10.1016/j.chemgeo.2012.01.028.
- Becker J. A., Bickle M. J., Galy A., and Holland T. J. B. (2008) Himalayan metamorphic CO₂ fluxes: Quantitative constraints from hydrothermal springs. *Earth Planet. Sci. Lett.* **265**, 616-629. doi:10.1016/j.epsl.2007.10.046.
- Berner E. K. and Berner R. A. (1996) *Global Environment: Water, Air, and Geochemical Cycles*. Prentice Hall. pp. 172-235.
- Beusen A. H. W., Bouwman A. F., Dürr H. H., Dekkers A. L. M., and Hartmann J. (2009) Global patterns of dissolved silica export to the coastal zone: Results from a spatially explicit global model. *Global Biogeochem. Cycles* **23**. doi:10.1029/2008gb003281.
- Blum J. D., Gazis C. A., Jacobsen A. D., and Chamberlain C. P. (1998) Carbonate versus silicate weathering in the Raikhot watershed within the High Himalayan Crystalline Series. *Geology* **26**, 411-414.
- Booth G., Raymond P., and Oh N.-H. (2007) *LoadRunner*. New Haven, CT. <http://environment.yale.edu/raymond/loadrunner>.
- Boyer E. W., Howarth R. W., Galloway J. N., Dentener F. J., Green P. A., and Vörösmarty C. J. (2006) Riverine nitrogen export from the continents to the coasts. *Global Biogeochem. Cycles* **20**. doi:10.1029/2005gb002537.
- Brisbin P. E. (1994) *Agricultural inventory of the Lower Fraser Valley data summary report. Management of livestock and poultry manures in the Lower Fraser Valley. Charcoal Creek Projects Inc., Abbotsford, B. C.*
- Calmels D., Galy A., Hovius N., Bickle M., West A. J., Chen M.-C., and Chapman H. (2011) Contribution of deep groundwater to the weathering budget in a rapidly eroding mountain belt, Taiwan. *Earth Planet. Sci. Lett.* **303**, 48-58. doi:10.1016/j.epsl.2010.12.032.
- Cameron E. M. (1996) Hydrogeochemistry of the Fraser River, British Columbia: seasonal variation in major and minor components. *J. Hydrol.* **182**, 209-225.

- Cameron E. M., Hall G. E. M., Veizer J., and Krouse H. R. (1995) Isotopic and elemental hydrogeochemistry of a major river system: Fraser River, British Columbia, Canada. *Chem. Geol.* **122**, 149-169.
- Cameron E. M. and Hattori K. (1997) Strontium and neodymium isotope ratios in the Fraser River, British Columbia: a riverine transect across the Cordilleran orogen. *Chem. Geol.* **137**, 243-253.
- Chao B. F., Wu Y. H., and Li Y. S. (2008) Impact of artificial reservoir water impoundment on global sea level. *Science* **320**, 212-214. doi:10.1126/science.1154580.
- Christophersen N., Neal C., Hooper R. P., Vogt R. D., and Andersen S. (1990) Modelling streamwater chemistry as a mixture of soilwater end-members — A step towards second-generation acidification models. *J. Hydrol.* **116**, 307-320.
- Coggins S. B., Coops N. C., Wulder M. A., Bater C. W., and Ortlepp S. M. (2011) Comparing the impacts of mitigation and non-mitigation on mountain pine beetle populations. *J. Environ. Manage.* **92**, 112-120. doi:10.1016/j.jenvman.2010.08.016.
- Cooper L. W., McClelland J. W., Holmes R. M., Raymond P. A., Gibson J. J., Guay C. K., and Peterson B. J. (2008) Flow-weighted values of runoff tracers ($\delta^{18}\text{O}$, DOC, Ba, alkalinity) from the six largest Arctic rivers. *Geophys. Res. Lett.* **35**. doi:10.1029/2008gl035007.
- Déry S. J., Hernández-Henríquez M. A., Owens P. N., Parkes M. W., and Petticrew E. L. (2012) A century of hydrological variability and trends in the Fraser River Basin. *Environ. Res. Lett.* **7**. doi:10.1088/1748-9326/7/2/024019.
- Dickson A. G., Sabine C. L., and Christian J. R. (2007) Guide to best practices for ocean CO_2 measurements. PICES Special Publication. Sidney, British Columbia, Canada. 191 pp.
- Dorcey A. H. J. (1991) Hydrology and water supply in the Fraser River basin. In *Water in Sustainable Development: Exploring Our Common Future in the Fraser River Basin* (eds. A. H. J. Dorcey and J. R. Griggs). Westwater Research Centre, Univ. of British Columbia, Vancouver, B.C. pp. 21-40.
- Dumont E., Harrison J. A., Kroeze C., Bakker E. J., and Seitzinger S. P. (2005) Global distribution and sources of dissolved inorganic nitrogen export to the coastal zone: Results from a spatially explicit, global model. *Global Biogeochem. Cycles* **19**. doi:10.1029/2005gb002488.
- Durum W. H., Heidel S. G., and Tison L. J. (1960) Worldwide run-off of dissolved solids. *IAHS-AISH Publ.* **51**, 618-628.
- Edmond J. M. (1992) Himalayan tectonics, weathering processes, and the strontium isotope record in marine limestones. *Science* **258**, 1594-1597.
- Fekete B. M., Vörösmarty C. J., and Grabs W. (2002) High-resolution fields of global runoff combining observed river discharge and simulated water balances. *Global Biogeochem. Cycles* **16**. doi:10.1029/1999GB001254.
- Friele P. A. and Clague J. J. (2009) Paraglacial geomorphology of Quaternary volcanic landscapes in the southern Coast Mountains, British Columbia. *Geol. Soc., London, Spec. Publ.* **320**, 219-233. doi:10.1144/sp320.14.
- Gaillardet J., Dupré B., Louvat P., and Allègre C. J. (1999) Global silicate weathering and CO_2 consumption rates deduced from the chemistry of large rivers. *Chem. Geol.* **159**, 3-30.
- Gaillardet J., Viers J., and Dupré B. (2003) Trace elements in river waters. In *Treatise on Geochemistry* (eds. H. D. Holland and K. K. Turekian). Elsevier. pp. 225-272.
- Galy A. and France-Lanord C. (1999) Weathering processes in the Ganges-Brahmaputra basin and the riverine alkalinity budget. *Chem. Geol.* **159**, 31-60.

- Gimeno L., Stohl A., Trigo R. M., Dominguez F., Yoshimura K., Yu L., Drumond A., Durán-Quesada A. M., and Nieto R. (2012) Oceanic and terrestrial sources of continental precipitation. *Rev. Geophys.* **50**. doi:10.1029/2012rg000389.
- Goldstein S. J. and Jacobsen S. B. (1987) The Nd and Sr isotopic systematics of river-water dissolved material: implications for the sources of Nd and Sr in seawater. *Chem. Geol.* **66**, 245-272.
- Graham S. T., Famiglietti J. S., and Maidment D. R. (1999) Five-minute, 1/2°, and 1° data sets of continental watersheds and river networks for use in regional and global hydrologic and climate system modeling studies. *Water Resour. Res.* **35**, 583-587. doi:10.1029/1998wr900068.
- Harrison J. A., Seitzinger S. P., Bouwman A. F., Caraco N. F., Beusen A. H. W., and Vörösmarty C. J. (2005) Dissolved inorganic phosphorus export to the coastal zone: Results from a spatially explicit, global model. *Global Biogeochem. Cycles* **19**. doi:10.1029/2004gb002357.
- Hartmann J., Jansen N., Dürr H. H., Kempe S., and Köhler P. (2009) Global CO₂-consumption by chemical weathering: What is the contribution of highly active weathering regions? *Global Planet. Change* **69**, 185-194. doi:10.1016/j.gloplacha.2009.07.007.
- Howarth R. W., Billen G., Swaney D., Townsend A., Jaworski N., Lajtha K., Downing J. A., Elmgren R., Caraco N., Jordan T., Berendse F., Freney J., Kudeyarov V., Murdoch P., and Zhao-Liang Z. (1996) Regional nitrogen budgets and riverine N & P fluxes for the drainages to the North Atlantic Ocean: Natural and human influences. *Biogeochemistry* **35**, 75-139.
- Huh Y., Birck J.-L., and Allègre C. J. (2004) Osmium isotope geochemistry in the Mackenzie River basin. *Earth Planet. Sci. Lett.* **222**, 115-129. doi:10.1016/j.epsl.2004.02.026.
- Hurwitz S., Evans W. C., and Lowenstern J. B. (2010) River solute fluxes reflecting active hydrothermal chemical weathering of the Yellowstone Plateau Volcanic Field, USA. *Chem. Geol.* **276**, 331-343. doi:10.1016/j.chemgeo.2010.07.001.
- IAEA/WMO (2006) Global Network of Isotopes in Precipitation. The GNIP Database. <http://www.iaea.org/water>.
- Kirchner J. W. and Neal C. (in press) Universal fractal scaling in stream chemistry and its implications for solute transport and water quality trend detection. *Proc. Natl. Acad. Sci.* doi:10.1073/pnas.1304328110.
- Liu Z., Kennedy C. D., and Bowen G. J. (2011) Pacific/North American teleconnection controls on precipitation isotope ratios across the contiguous United States. *Earth Planet. Sci. Lett.* **310**, 319-326. doi:10.1016/j.epsl.2011.08.037.
- Livingstone D. A. (1963) Chemical composition of rivers and lakes. In *Data of Geochemistry* (ed. M. Fleischer). United States Geological Survey, Washington D.C. pp. 1-64.
- Mackenzie F. T. and Garrels R. M. (1966) Chemical mass balance between rivers and oceans. *Am. J. Sci.* **264**, 507-525.
- Mayorga E., Seitzinger S. P., Harrison J. A., Dumont E., Beusen A. H. W., Bouwman A. F., Fekete B. M., Kroeze C., and Van Drecht G. (2010) Global Nutrient Export from WaterSheds 2 (NEWS 2): Model development and implementation. *Environ. Modell. Softw.* **25**, 837-853. doi:10.1016/j.envsoft.2010.01.007.
- Meybeck M. (1979) Concentrations des eaux fluviales en éléments majeurs et apports en solution aux océans. *Rev. Géol. Dyn. Géogr. Phys.* **21**, 215-246.

- Meybeck M. (1987) Global chemical weathering from surficial rocks estimated from river dissolved loads. *Am. J. Sci.* **287**, 401-428.
- Meybeck M. and Helmer R. (1989) The quality of rivers: from pristine stage to global pollution. *Palaeogeogr. Palaeoclimatol. Palaeoecol.* **75**, 283-309.
- Meybeck M. and Ragu A. (2012) GEMS-GLORI world river discharge database. Laboratoire de Géologie Appliquée, Université Pierre et Marie Curie, Paris.
doi:10.1594/PANGAEA.804574.
- Miller C. A. (2009) Surface-cycling of rhenium and its isotopes. PhD Thesis, Woods Hole Oceanog. Inst.
- Miller C. A., Peucker-Ehrenbrink B., Walker B. D., and Marcantonio F. (2011) Re-assessing the surface cycling of molybdenum and rhenium. *Geochim. Cosmochim. Acta* **75**, 7146-7179.
doi:10.1016/j.gca.2011.09.005.
- Milliman J. D., Farnsworth K. L., Jones P. D., Xu K. H., and Smith L. C. (2008) Climatic and anthropogenic factors affecting river discharge to the global ocean, 1951–2000. *Global Planet. Change* **62**, 187-194. doi:10.1016/j.gloplacha.2008.03.001.
- Millot R., Gaillardet J., Dupré B., and Allègre C. J. (2003) Northern latitude chemical weathering rates: clues from the Mackenzie River Basin, Canada. *Geochim. Cosmochim. Acta* **67**, 1305-1329. doi:10.1016/s0016-7037(02)01207-3.
- Morel F. M. M. and Hering J. G. (1993) *Principles and applications of aquatic chemistry*. John Wiley, Hoboken, N.J.
- Nilsson C. (2005) Fragmentation and flow regulation of the world's large river systems. *Science* **308**, 405-408. doi:10.1126/science.1107887.
- Northwest Hydraulic Consultants (2008) Comprehensive review of Fraser River at Hope flood hydrology and flows: scoping study. B.C. Ministry of Environment, North Vancouver, B.C. 1-25.
- Palmer M. R. and Edmond J. M. (1989) The strontium isotope budget of the modern ocean. *Earth Planet. Sci. Lett.* **92**, 11-26.
- Peterson B. J. (2006) Trajectory shifts in the Arctic and Subarctic freshwater cycle. *Science* **313**, 1061-1066. doi:10.1126/science.1122593.
- Peucker-Ehrenbrink B. and Miller M. W. (2007) Quantitative bedrock geology of the continents and large-scale drainage regions. *Geochem. Geophys. Geosyst.* **8**.
doi:10.1029/2006gc001544.
- Peucker-Ehrenbrink B., Miller M. W., Arsouze T., and Jeandel C. (2010) Continental bedrock and riverine fluxes of strontium and neodymium isotopes to the oceans. *Geochem. Geophys. Geosyst.* **11**. doi:10.1029/2009gc002869.
- Raymond P. A. and Cole J. J. (2003) Increase in the export of alkalinity from North America's largest river. *Science* **301**, 88-91. doi:10.1126/science.1083788.
- Runkel R. L., Crawford C. G., and Cohn T. A. (2004) Load Estimator (LOADEST): A FORTRAN program for estimating constituent loads in streams and rivers. U.S. Geological Survey techniques and methods Book 4, chapter A5. Reston, VA.
<http://water.usgs.gov/software/loadest>.
- Scanlon T. M., Raffensperger J. P., and Hornberger G. M. (2001) Modeling transport of dissolved silica in a forested headwater catchment: Implications for defining the hydrochemical response of observed flow pathways. *Water Resour. Res.* **37**, 1071-1082.
- Schulte P., van Geldern R., Freitag H., Karim A., Négrel P., Petelet-Giraud E., Probst A., Probst J.-L., Telmer K., Veizer J., and Barth J. A. C. (2011) Applications of stable water and

- carbon isotopes in watershed research: Weathering, carbon cycling, and water balances. *Earth-Sci. Rev.* **109**, 20-31. doi:10.1016/j.earscirev.2011.07.003.
- Seitzinger S. P., Harrison J. A., Dumont E., Beusen A. H. W., and Bouwman A. F. (2005) Sources and delivery of carbon, nitrogen, and phosphorus to the coastal zone: An overview of Global Nutrient Export from Watersheds (NEWS) models and their application. *Global Biogeochem. Cycles* **19**. doi:10.1029/2005gb002606.
- Shen Z.-L. and Liu Q. (2008) Nutrients in the Changjiang River. *Environ. Monit. Assess.* **153**, 27-44. doi:10.1007/s10661-008-0334-2.
- Spence J. and Telmer K. (2005) The role of sulfur in chemical weathering and atmospheric CO₂ fluxes: Evidence from major ions, $\delta^{13}\text{C}_{\text{DIC}}$, and $\delta^{34}\text{S}_{\text{SO}_4}$ in rivers of the Canadian Cordillera. *Geochim. Cosmochim. Acta* **69**, 5441-5458. doi:10.1016/j.gca.2005.07.011.
- Syvitski J. P. M. (2008) Deltas at risk. *Sustain. Sci.* **3**, 23-32. doi:10.1007/s11625-008-0043-3.
- Thorne R. and Woo M.-k. (2011) Streamflow response to climatic variability in a complex mountainous environment: Fraser River Basin, British Columbia, Canada. *Hydrol. Processes* **25**, 3076-3085. doi:10.1002/hyp.8225.
- Tipper E. T., Bickle M. J., Galy A., West A. J., Pomiès C., and Chapman H. J. (2006) The short term climatic sensitivity of carbonate and silicate weathering fluxes: Insight from seasonal variations in river chemistry. *Geochim. Cosmochim. Acta* **70**, 2737-2754. doi:10.1016/j.gca.2006.03.005.
- Wadleigh M. A., Veizer J., and Brooks C. (1985) Strontium and its isotopes in Canadian rivers: Fluxes and global implications. *Geochim. Cosmochim. Acta* **49**, 1727-1736.
- Walling D. E. and Foster I. D. L. (1975) Variations in the natural chemical concentration of river water during flood flows, and the lag effect: Some further comments. *J. Hydrol.* **26**, 237-244.
- Wang Z. A., Bienvenu D. J., Mann P. J., Hoering K. A., Poulsen J. R., Spencer R. G. M., and Holmes R. M. (2013) Inorganic carbon speciation and fluxes in the Congo River. *Geophys. Res. Lett.* **40**, 511-516. doi:10.1002/grl.50160.
- Wang Z. A. and Cai W.-J. (2004) Carbon dioxide degassing and inorganic carbon export from a marsh-dominated estuary (the Duplin River): A marsh CO₂ pump. *Limnol. Oceanogr.* **49**, 341-354.
- Wang Z. A., Voss B. M., Peucker-Ehrenbrink B., Eglinton T. I., and Hoering K. (in prep) Carbon cycling in the Fraser River, Canada: Inorganic carbon systematics.
- West A., Galy A., and Bickle M. (2005) Tectonic and climatic controls on silicate weathering. *Earth Planet. Sci. Lett.* **235**, 211-228. doi:10.1016/j.epsl.2005.03.020.
- Wheeler J. O., Hoffman P. F., Card K. D., Davidson A., Stanford B. V., Okulitch A. V., and Roest W. R. (1997) Geologic map of Canada, Map D1860A, version 1.0, scale 1:5,000,000. Nat. Resour. Can., Ottawa, Ont., Canada.
- Wolff-Boenisch D., Gabet E. J., Burbank D. W., Langner H., and Putkonen J. (2009) Spatial variations in chemical weathering and CO₂ consumption in Nepalese High Himalayan catchments during the monsoon season. *Geochim. Cosmochim. Acta* **73**, 3148-3170. doi:10.1016/j.gca.2009.03.012.